

We are thankful to the two reviewers for their thoughtful comments and suggestions that help improve the manuscript significantly. We have revised the manuscript accordingly. Listed below are our point-by-point responses in blue to each reviewer's comments

Response to reviewer #1

This manuscript reports one-year measurements of non-refractory submicron particles by Aerodyne Aerosol Chemical Speciation (ACSM) at an urban site in Beijing. Temporal variations of the particle concentration and composition as well as their associations with meteorological conditions are explored. The authors also provided footprint analyses for the potential source regions of aerosol components. Overall, this paper is well written and clearly describes the analysis. The paper addresses relevant scientific questions within the scope of ACP. Some results however seem to be over-interpreted and need additional constraints. New scientific findings also need more emphasis in comparison with previous work. I recommend this manuscript be published after the following specific comments are addressed.

Specific comments:

(1) In Abstract and Conclusion, it is not clear to me what the new findings are compared to previous studies.

We present the first long-term, highly time-resolved measurement of fine particle composition in Beijing, China. Compared to previous studies that either focused on limited aerosol species, relied upon weekly filter samples, or used one month's worth of data to represent an entire season (Zhang et al., 2013a; Zhang et al., 2013b), this study provides a full spectrum of seasonal variations and diurnal patterns of aerosol species in Beijing, China. This is important for a better understanding of the compositions, sources, and evolution processes of severe haze pollution among the different seasons and hence mitigating fine particle pollution in Beijing. New findings were also obtained in this study, for example, we observed insignificant seasonal variations of secondary inorganic aerosol which is different from the results reported in previous studies (Zhang et al., 2013a). The reasons for such inconsistency were elucidated in the manuscript. We also identified high potential source areas for different aerosol species during the four seasons which were rarely reported in previous studies. These results provide evidence and demonstrate the importance of regional transport in the formation of severe haze pollution in Beijing. In addition, we had a more comprehensive investigation of the meteorological effects, particularly relative humidity and temperature on the formation of different aerosol species with the advantage of 1 year data.

(2) Section 2.4: It is unclear how the footprints of air masses are converted to potential source concentrations of aerosol species. The authors should add a bit more details about the PSCF method.

Following the reviewer's comments, we expanded the PSCF method in section 2.4 in the revised manuscript.

(3) Page 14557, line 16-18: Many possible reasons can lead high mass concentration of NR-PM₁ in June compared to July and August. If the authors really think this is biomass burning impacts, they should provide evidence to prove, for example, fire product near the site or upwind. Mass spectral marks of biomass burning OA may also help.

Good point, we do have evidence. As shown in Fig. R1, a large number of fire spots were detected in north China plain including Beijing surrounding regions during the late June, suggesting the ubiquitous agricultural burning during the summer harvest season. In addition, PMF analysis was also performed on organic aerosol (OA) in June, and three factors including a biomass burning OA (BBOA) were identified (Fig. R2). The BBOA spectrum shows obvious m/z 60 and 73, which are two marker m/z 's for biomass burning (Alfarra et al., 2007; Cubison et al., 2011). Note that the signal intensities of m/z 60 and 73 were not as high as those from fresh biomass burning (Cubison et al., 2011), indicating that BBOA in this study was aged when transporting from surrounding regions to the Beijing city. The time series of BBOA in June (Fig. R2b) showed high concentrations during 18 – 22 June, further supporting the large impact of biomass burning on aerosol loadings.

Following the reviewer's suggestions, the plot of MODIS fire spots was added in supplementary to support our conclusions.

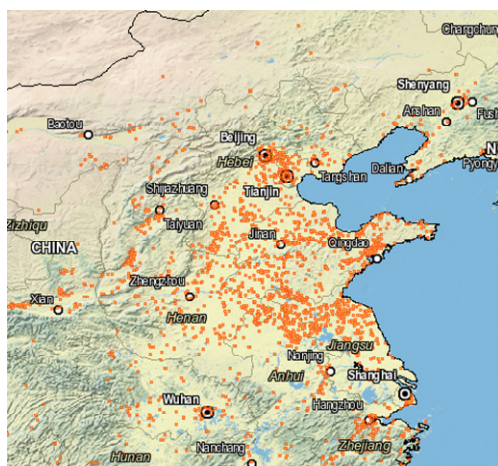


Fig. R1. Fire spots in north China plain during 15 – 30 June, 2012 (<https://firms.modaps.eosdis.nasa.gov/firemap/>).

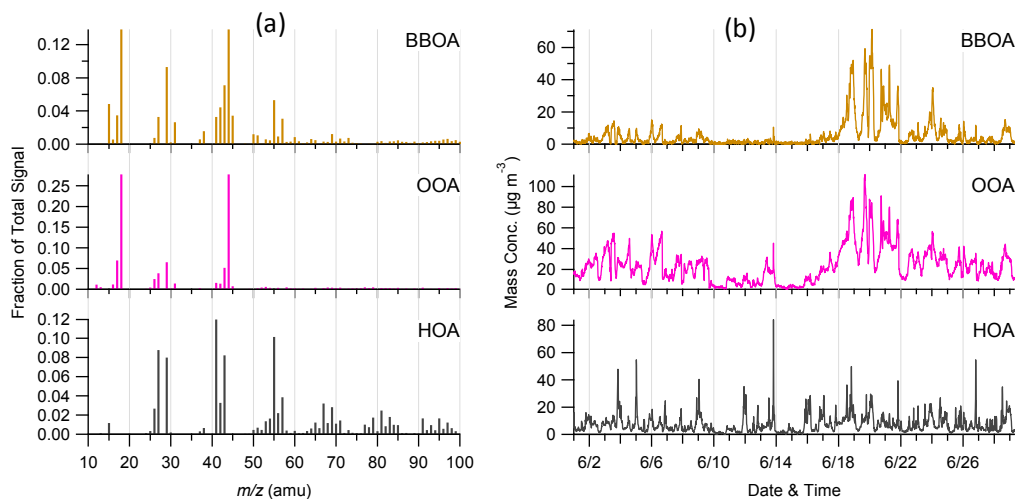


Fig. R2. (a) Mass spectra and (b) time series of three organic aerosol factors in June 2012.

(4) Page 14558, line 8-9: What are the definitions of moderately or heavy polluted days herein? Is it based on daily average, or day-time average, periodical spikes (e.g., plume) or consistent high NR-PM1 loadings? Figure 4 needs clarification about how the data is treated. High frequency of data points does not necessarily represent polluted days.

We thank the reviewer's comments. There was no exact definition for moderately and heavily polluted days. They were used for qualitative purpose which is $30 - 60 \mu\text{g m}^{-3}$ for moderately polluted days and $> 150 \mu\text{g m}^{-3}$ for heavily polluted days in this study. According to the Chinese National Ambient Air Quality Standard, it is defined as heavy pollution when the daily-average $\text{PM}_{2.5}$ concentration is above $250 \mu\text{g m}^{-3}$ (Air quality index = 300). Assuming that NR- PM_1 is approximately 60 % of $\text{PM}_{2.5}$, the NR- PM_1 concentration during heavily polluted days is expected to be $\sim 150 \mu\text{g m}^{-3}$. The frequency in Fig. 4 was calculated with 15 min average data. The major purpose of Fig. 4 is to investigate the frequency of different NR- PM_1 mass loadings during the four seasons, particularly the highly polluted events. This has important implications for health studies. Using daily average data could significantly underestimate the exposure of people in the time with high PM levels.

We agree with the reviewer that it's not accurate to use highly time-resolved data to describe "days". We revised this paragraph by changing "days" to "events", and also deleted "moderately polluted days" because of no accurate definition.

(5) Figures 3 and 4 show duplicate information. I suggest combining them into one figure.

We thank the reviewer's suggestion. Fig. 3 shows the time series of aerosol species and average chemical composition during four seasons, while Fig. 4 presents the frequency of NR- PM_1 mass loading for each season. We kept these two figures considering it is difficult to read when combining them into one figure.

(6) Page 14559, line 3-4 and page 14560, line 4-5: Similar to comment #3, the authors should provide evidence to support the conclusion that "due to the impacts of agricultural burning in these two months".

See our reply to comment #3.

(7) Page 14561, line 6: Is the particle-phase ammonium sufficient to neutralize inorganic species? It may be better to show the ion balance information to support the forms of inorganic species.

We checked the ammonium balance in winter by comparing the measured NH_4^+ with that requires to fully neutralize sulfate, nitrate, and chloride (Zhang et al., 2007). As shown in Fig. R3, aerosol particles in winter were overall neutralized ($\text{NH}_4^+_{\text{predicted}} / \text{NH}_4^+_{\text{measured}} = 0.93$) although periods with slight acid particles were also observed. Here we mainly address the effects of temperature on gas-particle partitioning of ammonium chloride in winter compared to other seasons, therefore we didn't show ion balance information in the manuscript.

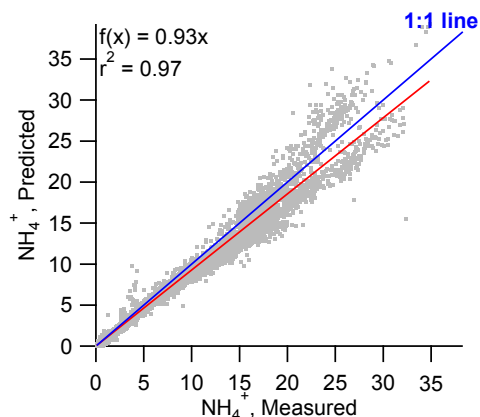


Fig. R3. Scatter plot of NH_4^+ predicted ($= 2 \times 18/96 \times \text{SO}_4^{2-} + 18/62 \times \text{NO}_3^- + 18/35.5 \times \text{Cl}^-$) vs. NH_4^+ measured in winter.

(8) Section 3.4: I am not convinced that the data for weekdays and weekend may really suggest anything about the emission strength without good constraints on meteorological conditions, atmospheric processing, and transport, life styles and so on in Beijing.

We agree with the reviewer that weekend effects can be affected by multiple factors including meteorological conditions, atmospheric processing, and even transport. However, for most of time, the meteorology conditions (temperature, relative humidity, and winds) and solar radiation won't change significantly in a week except special events, the comparisons between weekdays and weekends therefore could reflect, to some extent, the source emissions, e.g., primary aerosols, and also photochemical production of secondary species. In fact, such an approach has been widely used in many previous studies (Forster and Solomon, 2003; Pollack et al., 2012; Warneke et al., 2013; Wang et al., 2014). In this study, to better evaluate the weekend effects, the periods with low aerosol loadings ($\text{NR-PM}_{10} < 20 \mu\text{g m}^{-3}$) that were usually from different source areas compared to high mass loading periods, were excluded in the analysis, which can reduce the effects of meteorological conditions to a certain degree.

A more detailed evaluation of weekend effects needs to involve modeling work which is beyond the scope of this study.

Technical remarks: In-text citations should be displayed in a proper format, for example, should be "Sun et al., 2013a" instead of "Sun et al., 2013b" in page 14552, line 5 and "Zhang et al. (2013)" instead of "R. Zhang et al. (2013)" in line 27. First-name initials appeared in many other places, which should not.

The initials before some references in the text serve to distinguish this reference from other references with the same publication year, but a different first author with the same last name. Such a format is suggested by ACP.

Page 14553, line 6: Please provide references after "entire season".

The references Zhang et al. (2013b) and Zhang et al. (2013a) were provided.

Page 14553, line 15 and later text: The word "organics" doesn't exist in dictionary. Replace with "organic material" or "organic species".

Thanks the reviewer's suggestion. Considering "organics" is a common word that is widely used in the community, we keep it in the manuscript to be consistent with previous studies.

Page 14556, line 20: Metals are also refractory.

Yes, we revised this sentence as: "the ACSM cannot detect refractory black carbon, mineral dust, and metals."

Page 14558, line 2: Add "compared to other places in China" after "in Beijing".

Added.

Page 14560, line 25-26: Define "POA" and "SOA".

"POA" and "SOA" was defined in page 14553, line 17.

Page 14563, line 4: Replace "_ 8:00 until _19:00" by "about 8:00 to 19:00".

Replaced.

Response to reviewer #2

This manuscript reports results obtained with an Aerodyne Aerosol Chemical Speciation Monitor (ACSM) during a long-term measurement period (1 year) at Beijing, China. The authors describe the seasonal variations of non-refractory submicron particles (NR-PM1). Then, they discuss the properties of NR-PM1 as a function of the meteorological conditions and the air mass origin. This manuscript is very interesting and of prime importance, and is completely within the scope of Atmospheric Chemistry and Physics. Therefore, I highly recommend its publication after the authors address the following comments.

We are thankful to the reviewer for his/her positive comments on this manuscript.

Specific comments:

Page 14555, lines 5-20: when I read the calibration procedure of the ACSM in this paragraph and in the two first papers published by the group on this study (Sun et al., 2012; Sun et al., 2013), it seems that the RIE sulfate has not been calibrated with $(\text{NH}_4)_2\text{SO}_4$. This is important, because the RIE sulfate may vary a lot (up to a factor of 3) between different instruments. Therefore, if the default value has been used, there can be an important uncertainty on the accuracy of the sulfate concentrations. The authors can try to use the parameterization presented in Budisulistiorini et al. (2014) to estimate the RIE sulfate, and see if there is a high deviation from the default value. If it is the case, it can have an incidence on the $\text{NO}_3^-/\text{SO}_4^{2-}$ ratio discussed later by the authors (page 14559, lines 14-26).

The reviewer is right. We didn't calibrate ACSM with $(\text{NH}_4)_2\text{SO}_4$ in this study because such an approach was only proposed recently. Following the reviewer's suggestions, we checked the RIE_{SO_4} using the method presented in Budisulistiorini et al. (2014). The slopes of predicted SO_4^{2-} versus measured SO_4^{2-} varied from 0.95 to 1.41 during four seasons. As a result, the RIE of SO_4^{2-} varied from 1.1 to 1.6, leading to an uncertainty of 5% - 35% for sulfate quantification. Such an uncertainty is overall consistent with that (28%) from a recent comprehensive evaluation of ACSM measurements by Crenn et al. (2015). It should be noted that the approach suggested by Budisulistiorini et al. (2014) assumes that aerosol particles are fully neutralized. Considering that aerosol particle acidity in Beijing varied largely between different seasons (Liu, 2012), such a approach might introduce additional uncertainties for sulfate quantification. Therefore, we kept the default RIE of SO_4 in this study. Nevertheless, we expanded the discussions on RIE_{SO_4} in the experimental section 2.2, which helps readers know the uncertainties in sulfate quantification in this study.

Page 14561, lines 14-18: the authors mention that in winter, the sulfate concentration increased because of a significant increase of precursor SO_2 , which can be oxidized to form sulfate via either gas-phase oxidation or aqueous-phase processing. However, the RH was very low in winter (< 40%), compared to the other seasons, so maybe the aqueous-phase processing had a very limited influence on the sulfate formation in winter.

Thank the reviewer for pointing this out. Although the average RH for the entire winter was low, there were many episodes with high RH levels (> 60%) including fog events during wintertime, particularly when air masses were from the south (Sun et al., 2013b). SO_2 with high concentration can be rapidly oxidized to form sulfate via aqueous-phase processing (Sun et al., 2013a).

Page 14562, lines 8-19: there are a few discrepancies between the information given in this paragraph and PMF results presented in the two previous publications of the authors on this study. For instance, the authors mention that the noon peak of organics was primarily caused by cooking emissions, while the evening peak was driven by different primary emissions (cooking, traffic, and coal combustion emissions) among the different seasons. However, according to Sun et al. (2012), only OOA and HOA factors were identified in summer, no cooking or coal combustion related emissions. It is only in winter that the authors identified cooking and coal combustion organic aerosols (Sun et al., 2013). Obviously, the HOA factor identified in summer was a mixture of HOA and COA (Sun et al., 2012), but if the noon peaks, which were more significant in summer than in the other seasons, were mainly driven by cooking activities, a COA factor would certainly be easily identified in summer.

They were consistent. In summer, PMF analysis of the unit mass resolution (UMR) spectra cannot separate cooking aerosol from traffic-related HOA. This was similar to a study in summer 2006 in Beijing by a Quadrupole Aerosol Mass Spectrometer (Sun et al., 2010). The COA and traffic-related HOA were also not separated by PMF analysis of UMR spectra. The reasons for this might be either due to the similar spectra of COA and HOA that cannot be easily separated by PMF analysis of UMR spectra, or COA and HOA in summer are well mixed due to high temperature and turbulence. However, COA and HOA can be separated by PMF analysis of high resolution mass spectra of OA due to richer chemical information from ion fragments (Huang et al., 2010). Although COA is more significant in summer, it's unlikely to be resolved as an individual factor if UMR spectra are used for PMF analysis. Therefore, HOA in this case would be a mixture of traffic and cooking aerosols.

Coal combustion OA (CCOA) was only significant during the heating season. Indeed, CCOA was never resolved in summer in Beijing, even for the PMF analysis of high resolution mass spectra of OA (Huang et al., 2010), indicating that coal combustion is a minor source of OA in summer. In contrast, coal combustion OA can be easily resolved during wintertime due to substantial emissions for domestic heating (Sun et al., 2013b; Sun et al., 2014; Zhang et al., 2014).

Moreover, I am not sure to understand why cooking activities are reduced in winter (also mentioned on page 14565, lines 8-9). Normally, cooking activities should be more or less the same during the different seasons.

The largest difference in cooking activities between summer and winter is charbroiling. While charbroiling is popular at both noon and evening time in summer, it is significantly reduced in winter due to the low temperature outside.

Page 14563, lines 24-25: how did the authors determine that chloride was present under the form of ammonium chloride? In Sun et al. (2012), the authors mention that chloride measured by the ACSM is primarily ammonium chloride, since the ACSM does not detect sea salt. However, non refractory chlorides include also other compounds, such as HCl and organic chlorides. It should be very difficult to determine this point with the scatter plot of NH_4 measured vs NH_4 predicted, since the contribution of chloride to the total inorganic species is small compared to sulfate and nitrate.

Chloride mainly exists in the form of NH_4Cl because ACSM is insensitive to refractory NaCl and/or KCl at its vaporizer temperature of 600°C . There's possibility that chloride was also partly from HCl and organic chlorides. Organic chlorides could not make a large contribution to the total chloride since no organic chlorides were reported in Beijing aerosols to date.

ACSM detects particle phase chloride, whereas HCl is volatile, which has an equilibrium with NH_4Cl ($\text{NH}_4\text{Cl} \leftrightarrow \text{NH}_3 + \text{HCl}$). The chloride showed pronounced diurnal patterns with low concentration in the afternoon due to the evaporative loss of particle phase NH_4Cl to gas phase HCl. Therefore, chloride detected by the ACSM would be primarily ammonium chloride. We agree with the reviewer that it is difficult to distinguish the forms of chloride using ammonium balance plot.

We revised this sentence as “Chloride in this study was primarily detected as ammonium chloride because ACSM is insensitive to refractory NaCl and/or KCl at its vaporizer temperature of 600°C”

Technical corrections:

5) Page 14571, line 7: “in the formation of serve PM pollution”.

Corrected.

6) Figure 12: the text “(c) NO_3^- ” seems to be opaque, since it hides the label of the x-axis just on the top of it. Please make it transparent, or move it a little bit to the bottom.

Corrected.

Response to reviewer #3

Recommendation: Reject Reason: It has been stated clearly in "Aims and scope" of this journal that "The journal scope is focused on studies with general implications for atmospheric science rather than investigations that are primarily of local or technical interest." Apparently, this manuscript is a local interest in a single site of China.

We conducted the first long-term, highly time-resolved measurement of fine particle composition in Beijing, China. The formation mechanisms and evolution processes in driving the seasonal variations and diurnal cycles of aerosol species have general implications for atmospheric science. The impact of meteorological conditions (e.g., relative humidity and temperature) on aerosol formation mechanisms also has general implications for atmospheric community. In addition, the long-term data this study serves as an important contribution to modelers for evaluating regional and even global models. Also note that the air pollution in Beijing has attracted worldwide attention since the 2008 Olympic Games. Therefore we disagree with the reviewer that this manuscript is only a local interest, and we believe that our study fits well within the scope of ACP.

References:

- Alfarra, M. R., Prevot, A. S. H., Szidat, S., Sandradewi, J., Weimer, S., Lanz, V. A., Schreiber, D., Mohr, M., and Baltensperger, U.: Identification of the mass spectral signature of organic aerosols from wood burning emissions, *Environ. Sci. Technol.*, **41**, 5770-5777, 2007.
- Budisulistiorini, S. H., Canagaratna, M. R., Croteau, P. L., Baumann, K., Edgerton, E. S., Kollman, M. S., Ng, N. L., Verma, V., Shaw, S. L., Knipping, E. M., Worsnop, D. R., Jayne, J. T., Weber, R. J., and Surratt, J. D.: Intercomparison of an Aerosol Chemical Speciation Monitor (ACSM) with ambient fine aerosol measurements in downtown Atlanta, Georgia, *Atmos. Meas. Tech.*, **7**, 1929-1941, 10.5194/amt-7-1929-2014, 2014.
- Crenn, V., Sciare, J., Croteau, P. L., Verlhac, S., Fröhlich, R., Belis, C. A., Aas, W., Äijälä, M., Alastuey, A., Artiñano, B., Baisnée, D., Bonnaire, N., Bressi, M., Canagaratna, M., Canonaco, F., Carbone, C., Cavalli, F., Coz, E., Cubison, M. J., Esser-Gietl, J. K., Green, D. C., Gros, V., Heikkinen, L., Herrmann, H., Lunder, C., Minguillón, M. C., Močnik, G., O'Dowd, C. D., Ovadnevaite, J., Petit, J. E., Petralia, E., Poulain, L., Priestman, M., Riffault, V., Ripoll, A., Sarda-Estève, R., Slowik, J. G., Setyan, A., Wiedensohler, A., Baltensperger, U., Prévôt, A. S. H., Jayne, J. T., and Favez, O.: ACTRIS ACSM intercomparison – Part I: Reproducibility of concentration and fragment results from 13 individual Quadrupole Aerosol Chemical Speciation Monitors (Q-ACSM) and consistency with Time-of-Flight ACSM (ToF-ACSM), High Resolution ToF Aerosol Mass Spectrometer (HR-ToF-AMS) and other co-located instruments, *Atmos. Meas. Tech. Discuss.*, **8**, 7239-7302, 10.5194/amtd-8-7239-2015, 2015.
- Cubison, M. J., Ortega, A. M., Hayes, P. L., Farmer, D. K., Day, D., Lechner, M. J., Brune, W. H., Apel, E., Diskin, G. S., Fisher, J. A., Fuelberg, H. E., Hecobian, A., Knapp, D. J., Mikoviny, T.,

- Rierner, D., Sachse, G. W., Sessions, W., Weber, R. J., Weinheimer, A. J., Wisthaler, A., and Jimenez, J. L.: Effects of aging on organic aerosol from open biomass burning smoke in aircraft and laboratory studies, *Atmos. Chem. Phys.*, **11**, 12049-12064, 10.5194/acp-11-12049-2011, 2011.
- Forster, P. M. d. F., and Solomon, S.: Observations of a “weekend effect” in diurnal temperature range, *Proc. Natl. Acad. Sci. U.S.A.*, **100**, 11225-11230, 10.1073/pnas.2034034100, 2003.
- Huang, X. F., He, L. Y., Hu, M., Canagaratna, M. R., Sun, Y., Zhang, Q., Zhu, T., Xue, L., Zeng, L. W., Liu, X. G., Zhang, Y. H., Jayne, J. T., Ng, N. L., and Worsnop, D. R.: Highly time-resolved chemical characterization of atmospheric submicron particles during 2008 Beijing Olympic Games using an Aerodyne High-Resolution Aerosol Mass Spectrometer, *Atmos. Chem. Phys.*, **10**, 8933-8945, 10.5194/acp-10-8933-2010, 2010.
- Liu, Q.: Physical and chemical characteristics of submicron aerosol and its sources in Beijing, LAPC, Institute of Atmospheric Physics, Chinese Academy of Sciences, 2012.
- Pollack, I. B., Ryerson, T. B., Trainer, M., Parrish, D. D., Andrews, A. E., Atlas, E. L., Blake, D. R., Brown, S. S., Commane, R., Daube, B. C., de Gouw, J. A., Dubé, W. P., Flynn, J., Frost, G. J., Gilman, J. B., Grossberg, N., Holloway, J. S., Kofler, J., Kort, E. A., Kuster, W. C., Lang, P. M., Lefer, B., Lueb, R. A., Neuman, J. A., Nowak, J. B., Novelli, P. C., Peischl, J., Perring, A. E., Roberts, J. M., Santoni, G., Schwarz, J. P., Spackman, J. R., Wagner, N. L., Warneke, C., Washenfelder, R. A., Wofsy, S. C., and Xiang, B.: Airborne and ground-based observations of a weekend effect in ozone, precursors, and oxidation products in the California South Coast Air Basin, *J. Geophys. Res.*, **117**, D00V05, 10.1029/2011jd016772, 2012.
- Sun, J., Zhang, Q., Canagaratna, M. R., Zhang, Y., Ng, N. L., Sun, Y., Jayne, J. T., Zhang, X., Zhang, X., and Worsnop, D. R.: Highly time- and size-resolved characterization of submicron aerosol particles in Beijing using an Aerodyne Aerosol Mass Spectrometer, *Atmos. Environ.*, **44**, 131-140, 2010.
- Sun, Y. L., Wang, Z., Fu, P., Jiang, Q., Yang, T., Li, J., and Ge, X.: The impact of relative humidity on aerosol composition and evolution processes during wintertime in Beijing, China, *Atmos. Environ.*, **77**, 927–934, <http://dx.doi.org/10.1016/j.atmosenv.2013.06.019>, 2013a.
- Sun, Y. L., Wang, Z. F., Fu, P. Q., Yang, T., Jiang, Q., Dong, H. B., Li, J., and Jia, J. J.: Aerosol composition, sources and processes during wintertime in Beijing, China, *Atmos. Chem. Phys.*, **13**, 4577-4592, 10.5194/acp-13-4577-2013, 2013b.
- Sun, Y. L., Jiang, Q., Wang, Z., Fu, P., Li, J., Yang, T., and Yin, Y.: Investigation of the sources and evolution processes of severe haze pollution in Beijing in January 2013, *J. Geophys. Res.*, **119**, 4380-4398, 10.1002/2014JD021641, 2014.
- Wang, Y. H., Hu, B., Ji, D. S., Liu, Z. R., Tang, G. Q., Xin, J. Y., Zhang, H. X., Song, T., Wang, L. L., Gao, W. K., Wang, X. K., and Wang, Y. S.: Ozone weekend effects in the Beijing–Tianjin–Hebei metropolitan area, China, *Atmos. Chem. Phys.*, **14**, 2419-2429, 10.5194/acp-14-2419-2014, 2014.
- Warneke, C., de Gouw, J. A., Edwards, P. M., Holloway, J. S., Gilman, J. B., Kuster, W. C., Graus, M., Atlas, E., Blake, D., Gentner, D. R., Goldstein, A. H., Harley, R. A., Alvarez, S., Rappenglueck, B., Trainer, M., and Parrish, D. D.: Photochemical Aging of Volatile

- Organic Compounds in the Los Angeles Basin: Weekday - Weekend Effect, *Journal of Geophysical Research: Atmospheres*, n/a-n/a, 10.1002/jgrd.50423, 2013.
- Zhang, J. K., Sun, Y., Liu, Z. R., Ji, D. S., Hu, B., Liu, Q., and Wang, Y. S.: Characterization of submicron aerosols during a month of serious pollution in Beijing, 2013, *Atmos. Chem. Phys.*, 14, 2887-2903, 10.5194/acp-14-2887-2014, 2014.
- Zhang, Q., Jimenez, J. L., Worsnop, D. R., and Canagaratna, M.: A case study of urban particle acidity and its effect on secondary organic aerosol, *Environ. Sci. Technol.*, 41, 3213-3219, 2007.
- Zhang, R., Jing, J., Tao, J., Hsu, S. C., Wang, G., Cao, J., Lee, C. S. L., Zhu, L., Chen, Z., Zhao, Y., and Shen, Z.: Chemical characterization and source apportionment of PM_{2.5} in Beijing: seasonal perspective, *Atmos. Chem. Phys.*, 13, 7053-7074, 10.5194/acp-13-7053-2013, 2013a.
- Zhang, Y., Sun, J., Zhang, X., Shen, X., Wang, T., and Qin, M.: Seasonal characterization of components and size distributions for submicron aerosols in Beijing, *Sci. China Earth Sci.*, 56, 890 - 900, 10.1007/s11430-012-4515-z, 2013b.

1 Long-term real-time measurements of aerosol particle composition in
2 Beijing, China: seasonal variations, meteorological effects, and source
3 analysis

4
5 Y. L. Sun^{1*}, Z. F. Wang¹, W. Du^{1,2}, Q. Zhang³, Q. Q. Wang¹, P. Q. Fu¹, X. L. Pan⁴, J. Li¹,
6 J. Jayne⁵, D. R. Worsnop⁵

7
8 *¹State Key Laboratory of Atmospheric Boundary Layer Physics and Atmospheric
9 Chemistry, Institute of Atmospheric Physics, Chinese Academy of Sciences, Beijing
10 100029, China*

11 *²Department of Resources and Environment, Air Environmental Modeling and Pollution
12 Controlling Key Laboratory of Sichuan Higher Education Institutes, Chengdu University
13 of Information Technology, Chengdu 610225, China*

14 *³Department of Environmental Toxicology, University of California, 1 Shields Ave.,
15 Davis, CA 95616*

16 *⁴Research Institute for Applied Mechanics, Kyushu University, Fukuoka, Japan*

17 *⁴Aerodyne Research, Inc., Billerica, MA 01821, USA*

18

19 *Correspondence to Y. L. Sun (sunyele@mail.iap.ac.cn)

20 **Abstract**

21 High concentrations of fine particles ($PM_{2.5}$) are frequently observed during all seasons in
22 Beijing, China, leading to severe air pollution and human health problems in this
23 megacity. In this study, we conducted real-time measurements of non-refractory
24 submicron aerosol (NR- PM_1) species (sulfate, nitrate, ammonium, chloride, and organics)
25 in Beijing using an Aerodyne Aerosol Chemical Speciation Monitor for 1 year, from July
26 2011 to June 2012. This is the first long-term, highly time-resolved (~ 15 min)
27 measurement of fine particle composition in China. The seasonal average ($\pm 1\sigma$) mass
28 concentration of NR- PM_1 ranged from $52 (\pm 49) \mu\text{g m}^{-3}$ in the spring season to $62 (\pm 49)$
29 $\mu\text{g m}^{-3}$ in the summer season, with organics being the major fraction (40–51%), followed
30 by nitrate (17–25%) and sulfate (12–17%). Organics and chloride showed pronounced
31 seasonal variations, with much higher concentrations in winter than in the other seasons,
32 due to enhanced coal combustion emissions. Although the seasonal variations of
33 secondary inorganic aerosol (SIA = sulfate + nitrate + ammonium) concentrations were
34 not significant, higher contributions of SIA were observed in summer (57–61%) than in
35 winter (43–46%), indicating that secondary aerosol production is a more important
36 process than primary emissions in summer. Organics presented pronounced diurnal
37 cycles that were similar among all seasons, whereas the diurnal variations of nitrate were
38 mainly due to the competition between photochemical production and gas–particle
39 partitioning. Our data also indicate that high concentrations of NR- PM_1 ($> 60 \mu\text{g m}^{-3}$) are
40 usually associated with high ambient relative humidity (RH) ($> 50\%$) and that severe
41 particulate pollution is characterized by different aerosol composition in different
42 seasons. All NR- PM_1 species showed evident concentration gradients as a function of
43 wind direction, generally with higher values associated with wind from the south,
44 southeast or east. This was consistent with their higher potential as source areas, as
45 determined by potential source contribution function analysis. A common high potential
46 source area, located to the southwest of Beijing along the Taihang Mountains, was
47 observed during all seasons except winter, when smaller source areas were found. These
48 results demonstrate a high potential impact of regional transport from surrounding
49 regions on the formation of severe haze pollution in Beijing.

50 **1 Introduction**

51 Severe haze pollution episodes, characterized by high concentrations of fine particles
52 ($\text{PM}_{2.5}$), occur frequently during all seasons in China (Sun et al., 2013b; Guo et al., 2014;
53 Zheng et al., 2015), not only reducing visibility significantly, but also exerting harmful
54 effects on public health (Cao et al., 2012). The mass concentrations of $\text{PM}_{2.5}$ often far
55 exceed the China National Ambient Air Quality Standard (NAAQS; $75 \mu\text{g m}^{-3}$ as a 24-
56 hour average), particularly in the economically developed regions of Beijing–Tianjin–
57 Hebei and Yangtze River Delta (YRD). According to Beijing Environmental Statements,
58 the annual average mass concentration of $\text{PM}_{2.5}$ was 89.5 and $85.9 \mu\text{g m}^{-3}$ in 2013 and
59 2014, respectively, 2.5 times the NAAQS ($35 \mu\text{g m}^{-3}$ as an annual average), indicating
60 that Beijing is still facing severe fine particle pollution. While extensive studies have
61 been conducted in recent years to characterize severe haze pollution (e.g., Guo et al.,
62 2014; Huang et al., 2014; Sun et al., 2014; Zheng et al., 2015), most were carried out in a
63 particular season. In reality, the very different compositions, sources, and evolution
64 processes of severe haze pollution among the different seasons mean that a longer-term
65 approach is needed to meet the challenge of mitigating fine particle pollution in Beijing.

66 A number of long-term measurements and source analyses have been conducted in
67 Beijing during the last decade. Zhao et al. (2009) reported pronounced seasonal variations
68 of $\text{PM}_{2.5}$, with higher concentrations in winter than summer. Similarly, Yang et al. (2011)
69 conducted a long-term study of carbonaceous aerosol from 2005 to 2008 in urban
70 Beijing. Both organic carbon (OC) and elemental carbon (EC) showed pronounced
71 seasonal variations, with the highest concentrations occurring in winter and the lowest
72 values in summer. A more detailed investigation of the chemical composition and sources
73 of $\text{PM}_{2.5}$ in urban Beijing can be found in Zhang et al. (2013a). Sources of fine particles
74 also vary greatly among the different seasons; for instance, coal combustion during
75 periods requiring more domestic heating, biomass burning in harvest seasons, and dust
76 storms in spring (Zheng et al., 2005; Zhang et al., 2013a). Despite this, most previous
77 long-term studies either focused on limited aerosol species, relied upon weekly filter
78 samples, or used one month's worth of data to represent an entire season (Zhang et al.,
79 2013a; Zhang et al., 2013b). Therefore, our understanding of the full spectrum of
80 seasonal variations of aerosol species and sources remains quite poor.

81 The Aerodyne Aerosol Mass Spectrometer (AMS) is unique in its ability to provide
82 real-time, online measurements of size-resolved submicron aerosol composition (Jayne et
83 al., 2000; Canagaratna et al., 2007). While the AMS has been widely used in China in
84 recent years (Xu et al., 2014a and references therein), real-time, long-term measurements
85 of aerosol particle composition are still rare. Zhang et al. (2013b) conducted a four-month
86 measurement campaign of submicron aerosol composition and size distributions using a
87 quadrupole AMS in urban Beijing. Their results showed higher concentration of organics
88 during wintertime and secondary inorganic species in summer. Furthermore, positive
89 matrix factorization (PMF) analysis of organic aerosol (OA) showed higher primary OA
90 (POA) in winter and secondary OA (SOA) in summer. However, measurements over
91 only one month or even less were conducted for each season, due to the high cost and
92 maintenance of the AMS. The recently developed Aerosol Chemical Speciation Monitor
93 (ACSM) is specially designed for long-term routine measurements of submicron aerosol
94 composition (Ng et al., 2011). The ACSM has been proven reliable by several recent
95 long-term field measurements, e.g., in Paris (Petit et al., 2015), north-central Oklahoma
96 (Parworth et al., 2015), and Santiago de Chile (Carbone et al., 2013). Although the
97 ACSM has been deployed at various sites in China (Sun et al., 2012; Sun et al., 2013b;
98 Zhang et al., 2015), long-term measurements have yet to be reported.

99 In this study, the first of its kind, we conducted long-term, real-time measurements of
100 non-refractory submicron aerosol (NR-PM₁) composition with an ACSM in Beijing,
101 China, from July 2011 to June 2012. The seasonal variations of mass concentration and
102 composition of submicron aerosol were characterized, and the diurnal cycles of aerosol
103 species during the four seasons elucidated. The effects of meteorological parameters,
104 particularly relative humidity and temperature, on aerosol composition and formation
105 mechanisms were investigated. Finally, the potential source areas leading to high
106 concentrations of aerosol species during the four seasons were investigated via potential
107 source contribution function (PSCF) analysis.

108 **2 Experimental methods**

109 **2.1 Sampling site**

110 The ACSM was deployed on the roof of a two-story building (~8 m) at the Institute of

111 Atmospheric Physics (IAP), Chinese Academy of Sciences (39°58'28''N, 116°22'16''E,
112 | **FigureFig.** 1a) from July 2011 to June 2012. The sampling site is located between the
113 north third and fourth ring road in Beijing, which is a typical urban site with influences
114 | from local traffic and cooking sources (Sun et al., 2012). The wind rose plots (**FigureFig.**
115 1b) show that southwesterly winds dominate all seasons except winter, when
116 northwesterly and northerly winds prevail. The spring and fall seasons are also
117 characterized by high frequencies of northwesterly and northerly winds. Also note that
118 the prevailing winds with high wind speeds are more frequent during winter and spring
119 than summer.

120 The meteorological parameters, including wind speed (WS), wind direction, relative
121 humidity (RH), and temperature (T) were obtained from a 325 m meteorological tower at
122 the same location. The parameters of pressure (P), solar radiation (SR), and precipitation
123 were obtained from a ground meteorological station located nearby. The monthly
124 | variations of these meteorological parameters are presented in **FigureFig.** 2. Pronounced
125 seasonal variations were observed for all meteorological parameters except WS. RH
126 averaged at $>\sim 60\%$ in summer and presented its minimum value ($< 30\%$) in February.
127 Temperature and solar radiation showed similar seasonal cycles, with high values in
128 summer and low values in winter. The monthly variations of WS were relatively flat, yet
129 slightly higher values in spring were observed. In addition, a considerable amount of
130 precipitation was observed from June to August, yet it was negligible during wintertime.

131 **2.2 Aerosol and gas measurements**

132 The submicron aerosol particle composition including organics, sulfate, nitrate,
133 ammonium, and chloride was measured *in-situ* by the ACSM at a time resolution of ~ 15
134 min. The ACSM, built upon previous AMSs (Jayne et al., 2000; Drewnick et al., 2005;
135 DeCarlo et al., 2006), is specially designed for long-term routine measurements of fine
136 particle composition (Ng et al., 2011). The ACSM has been successfully deployed at
137 various sites for chemical characterization of submicron aerosol (Ng et al., 2011;
138 Budisulistiorini et al., 2013; Carbone et al., 2013; Sun et al., 2013b; Parworth et al.,
139 2015). In this study, ambient aerosol particles were delivered to the sampling room
140 through a stainless steel tubing (outer diameter: 1.27 cm) with a flow rate of $\sim 3 \text{ L min}^{-1}$,

141 out of which $\sim 84 \text{ cc min}^{-1}$ was sampled into the ACSM. A $\text{PM}_{2.5}$ URG cyclone (URG-
142 2000-30ED) was installed in front of the sampling line to remove coarse particles (> 2.5
143 μm). To reduce the uncertainties of collection efficiency (CE), a silica gel diffusion dryer
144 was set up in the front of the ACSM to ensure that the aerosol particles sampled were dry
145 ($< 40\%$). The ACSM was calibrated routinely with pure ammonium nitrate particles for
146 the response factor following the procedures detailed in Ng et al. (2011). A more detailed
147 description of the ACSM calibration is also given in Sun et al. (2012). **It should be noted**
148 **that we didn't calibrate the ACSM with $(\text{NH}_4)_2\text{SO}_4$ to determine the relative ionization**
149 **efficiency (RIE) of sulfate since such an approach was only proposed recently. Using the**
150 **method suggested by Budisulistiorini et al. (2014), the RIE of sulfate was estimated to be**
151 **1.1 – 1.6 during four seasons, leading to a highest uncertainty of 35% in sulfate**
152 **quantification. Considering that aerosol particle acidity may vary largely between**
153 **different seasons, the method of Budisulistiorini et al. (2014) may introduce additional**
154 **uncertainties in sulfate quantification. Therefore, we kept the default RIE of sulfate for**
155 **the data analysis in this study.**

156 **2.3 ACSM data analysis**

157 The ACSM data were analyzed for the mass concentrations of NR- PM_1 species
158 including organics, sulfate, nitrate, ammonium, and chloride using ACSM standard data
159 analysis software. The RH in the sampling line, aerosol particle acidity and the fraction of
160 ammonium nitrate (f_{AN}) in NR- PM_1 are three major factors affecting the uncertainties of
161 CE (Huffman et al., 2005; Matthew et al., 2008; Middlebrook et al., 2012). Because
162 aerosol particles were dry and overall neutralized for most of the time, except some
163 periods when the ratio of measured NH_4^+ to predicted NH_4^+ ($= 2 \times \text{SO}_4^{2-} / 96 \times 18 +$
164 $\text{NO}_3^- / 62 \times 18 + \text{Cl}^- / 35.5 \times 18$) (Zhang et al., 2007) was less than 0.8, the composition
165 dependent CE recommended by Middlebrook et al. (2012), which is $\text{CE} = \max(0.45,$
166 $0.0833 + 0.9167 \times f_{\text{AN}})$, was used in this study. The validity of the ACSM data using
167 variable CE in summer and winter was reported previously in Sun et al. (2012) and Sun
168 et al. (2013b) by comparing the NR- PM_1 with $\text{PM}_{2.5}$ mass concentration measured by a
169 TEOM system. The correlation between NR- PM_1 and $\text{PM}_{2.5}$ for the entire year is shown
170 in **FigureFig. S1**. The measured NR- PM_1 overall tracked well with that of $\text{PM}_{2.5}$, and yet
171 showed different slopes in different seasons. The average ratio of NR- $\text{PM}_1/\text{PM}_{2.5}$ for the

172 entire year was 0.77 ($r^2 = 0.66$). It should be noted that the $PM_{2.5}$ was measured by a
173 heated TEOM (50°C), which might have caused significant losses of semi-volatile
174 species, e.g., ammonium nitrate and semi-volatile organics. For example, Docherty et al.
175 (2011) found an average loss of ~44% $PM_{2.5}$ mass through use of the heated TEOM
176 compared to that measured with a filter dynamics measurement system. Assuming that
177 the average loss of $PM_{2.5}$ mass by the heated TEOM is 30–50%, the NR- $PM_1/PM_{2.5}$ ratio
178 for the entire study would be ~0.5–0.6, which is close to that reported in Zhang et al.
179 (2013b). Figure S1 also shows large variations of NR- $PM_1/PM_{2.5}$ ratios in the different
180 seasons. The reasons for the variations include: 1) the ACSM cannot detect refractory
181 black carbon ~~and~~, mineral dust, ~~and~~ metals. For example, low ratios of NR- $PM_1/PM_{2.5}$ (<
182 0.3) were observed during dust storm periods, when mineral dust is the dominant
183 component of fine particles; 2) the contribution of semi-volatile species to $PM_{2.5}$ varied
184 greatly among the different seasons; and 3) the contribution of particles in the range of 1–
185 2.5 μm to the total $PM_{2.5}$ might also be different among different pollution episodes.

186 2.4 PSCF analysis

187 The 72 hr back trajectories arriving at the IAP study site at a height of 300 m were
188 calculated every 3 hr for the entire study period using the National Oceanic and
189 Atmospheric Administration Hybrid Single-Particle Lagrangian Integrated Trajectory
190 model, version 4.8 (Draxler and Rolph, 2003). Each trajectory contained a series of
191 latitude-longitude coordinates every 1 h backward in time for 72 hr. If a trajectory end
192 point falls into a grid cell (i, j), the trajectory is assumed to collect material emitted in the
193 cell (Polissar, 1999). The number of end points falling into a single grid cell is n_{ij} . Some
194 of these trajectory end points are associated with the data with the concentration of
195 aerosol species higher than a threshold value. The number of these points is m_{ij} . The
196 potential source contribution function (PSCF) is then calculated as ~~The back trajectory~~
197 ~~data were then input into the PSCF, which calculates~~ the ratio of the number of points
198 with concentration higher than a threshold value (m_{ij}) to the total number of points (n_{ij}) in
199 the ij -th grid cell. Higher PSCF values indicate higher potential source contributions to
200 the receptor site. In this study, the domain for the PSCF was set in the range of (34–44°N,
201 110–124°E). The 75th percentile for each aerosol species during the four seasons (Table
202 S1) was used as the threshold value to calculate m_{ij} . To reduce the uncertainties of m_{ij}/n_{ij}

203 for those grid cells with a limited number of points, a weighting function (w_{ij})
204 recommended by Polissar et al. (1999) was applied to the PSCF in each season.

$$w_{ij} = \begin{cases} 1.00 & 80 < n_{ij} \\ 0.70 & 20 < n_{ij} \leq 80 \\ 0.42 & 10 < n_{ij} \leq 20 \\ 0.05 & n_{ij} \leq 10 \end{cases}$$

205 3 Results and discussion

206 3.1 Mass concentration and chemical composition

207 The average mass concentration of NR-PM₁ was 62 $\mu\text{g m}^{-3}$ in summer (FigureFig. 3),
208 which is higher than the 50 $\mu\text{g m}^{-3}$ for July–August 2011 reported in Sun et al. (2012)
209 due to the biomass burning impacts in June 2012 (Fig. S2). The summer NR-PM₁ level is
210 close to that measured by a High Resolution Aerosol Mass Spectrometer during the
211 Beijing 2008 Olympic Games (Huang et al., 2010), but ~20% lower than that determined
212 in summer 2006 (Sun et al., 2010). The average NR-PM₁ mass concentrations were
213 relatively similar during the other three seasons, varying from 52 to 59 $\mu\text{g m}^{-3}$ and with
214 slightly higher concentration during wintertime (FigureFig. 3). The NR-PM₁ measured in
215 urban Beijing is overall higher than those previously reported in the Yangtze River Delta
216 (YRD) region (27–43 $\mu\text{g m}^{-3}$) (Huang et al., 2012; Huang et al., 2013; Zhang et al., 2015)
217 and Pearl River Delta (PRD) region (31–48 $\mu\text{g m}^{-3}$) (He et al., 2011; Huang et al., 2011;
218 Gong et al., 2012), indicating more severe submicron aerosol pollution in Beijing
219 compared to other places in China. Indeed, the annual average NR-PM₁ concentration (57
220 $\mu\text{g m}^{-3}$) was much higher than the China NAAQS of PM_{2.5} (35 $\mu\text{g m}^{-3}$ as an annual
221 average). Assuming a similar PM_{2.5} level as that (89.5 $\mu\text{g m}^{-3}$) in Beijing in 2013, NR-
222 PM₁ on average accounted for 64% of PM_{2.5}, which is overall consistent with the results
223 reported in previous studies (Sun et al., 2012; Sun et al., 2013b; Zhang et al., 2013b).

224 As indicated in FigureFig. 4, the summer season showed the highest frequency of
225 moderately polluted days, with NR-PM₁ loading in the range of 30–60 $\mu\text{g m}^{-3}$ (36% of
226 the time), while the winter season presented the highest frequency of low mass loadings
227 (< 20 $\mu\text{g m}^{-3}$, 34% of the time) due to the prevailing northwesterly winds (FigureFig.
228 1b). However, high NR-PM₁ loading (> 90 $\mu\text{g m}^{-3}$) occurred 31% of the time during the

229 winter season, substantially more than during any of the other seasons (25%, 25% and
230 21% during summer, fall and spring, respectively), indicating that heavy pollution
231 occurred more frequently during winter than the other seasons. The fall and spring
232 seasons showed similar variations of frequencies, which overall decreased monotonically
233 as a function of NR-PM₁ loadings. Note that heavily polluted ~~day~~events, with NR-PM₁
234 mass concentrations larger than 150 μg m⁻³, occurred during all seasons, on average
235 accounting for 3–7% of the total time. Such heavily polluted ~~days~~events were mainly
236 caused by agricultural burning in summer and fall, and coal combustion in winter,
237 particularly under stagnant meteorological conditions (Sun et al., 2013b; Cheng et al.,
238 2014).

239 The NR-PM₁ species varied dramatically and differently during the four seasons
240 (~~Figure~~Fig. 3). Overall, organics dominated NR-PM₁ during all seasons, accounting for
241 40–51% on average. The dominance of organics in NR-PM₁ has been widely observed at
242 various sites in China, e.g., 31–52% in the YRD region (Huang et al., 2012; Huang et al.,
243 2013; Zhang et al., 2015), 36–46% in the PRD region (He et al., 2011; Huang et al.,
244 2011; Gong et al., 2012), and 47% in northwest China (Xu et al., 2014a). Organics
245 showed the largest contribution to NR-PM₁ in winter due to a large amount of
246 carbonaceous aerosol emitted from coal combustion (Chen et al., 2005; Zhang et al.,
247 2008). This is also consistent with the highest contribution of chloride, with coal
248 combustion being a major source in winter (Zhang et al., 2012). High concentrations of
249 organics were also observed during late June and ~~late~~early October, due to the impacts of
250 agricultural burning in these two months. Secondary inorganic aerosol (SIA = sulfate +
251 nitrate + ammonium) contributed the largest fraction of NR-PM₁ during the summer
252 season (59%) and the lowest fraction during the winter season (44%). Such seasonal
253 differences in PM composition reflect the different roles played by primary emissions and
254 secondary formation. While photochemical production of secondary aerosol associated
255 with higher O₃ and stronger solar radiation (~~Figure~~Fig. 2) plays a dominant role in
256 affecting aerosol composition in summer, primary emissions play enhanced roles in
257 winter when photochemical processing is weaker (Sun et al., 2013b). It is interesting to
258 note that nitrate, on average, showed a higher contribution than sulfate during the four
259 seasons. Compared to previous AMS measurements in Beijing (Huang et al., 2010; Sun

260 et al., 2010), the nitrate contribution to NR-PM₁ appears to show an increasing trend. The
261 ratio of NO₃⁻/SO₄²⁻ varied from 1.3–1.8 in this study, which is overall higher than those
262 (0.8–1.5) observed during the four seasons in 2008 (Zhang et al., 2013b). This result
263 likely indicates a response of secondary inorganic aerosol composition to the variations
264 of precursors of NO_x and SO₂ in recent years. For instance, a continuous effort to reduce
265 SO₂ emissions is accompanied with a gradual increase in NO_x emissions (Wang et al.,
266 2014b), which results in an increasingly more important role played by nitrate in PM
267 pollution in Beijing. Indeed, a recent model analysis of the response of SIA to their
268 precursors from 2000–2015 showed that the increase of nitrate would exceed the
269 reduction of sulfate in northern China, assuming no change to NH₃ emissions (Wang et
270 al., 2013). A higher concentration of nitrate than sulfate has also been frequently
271 observed at urban and rural sites in China in recent years, e.g., Nanjing, in the YRD
272 region (Zhang et al., 2015), and Changdao Island (Hu et al., 2013).

273 3.2 Seasonal variations

274 The monthly average NR-PM₁ mass concentration stayed relatively constant
275 throughout the year, with the average value ranging from 46 to 60 μg m⁻³, except in June
276 | 2012 (FigureFig. 5). The month of June presented the highest NR-PM₁ (89 μg m⁻³) due
277 | to the impact of agricultural burning. Consistently, a higher concentration of NR-PM₁
278 was observed in the summer of 2008 (5 June – 3 July) than the other seasons in Beijing
279 (Zhang et al., 2013b). Zhao et al. (2009) also observed the highest concentration of PM_{2.5}
280 in June 2007, due to the influences of agricultural burning. These results indicate that
281 agricultural burning is a large source of PM pollution in Beijing in summer. The lowest
282 concentration of NR-PM₁ in this study occurred in July, mainly due to the abundant
283 precipitation and high temperatures, which facilitated wet scavenging and convection of
284 | PM, respectively (FigureFig. 2). Similarly lower concentrations of PM_{2.5} in summer than
285 | in the other seasons were also observed previously at an urban site in Beijing (Zhao et al.,
286 | 2009).

287 Among the NR aerosol species, organics and chloride presented pronounced seasonal
288 | variations, showing higher concentrations in winter than the other seasons (FigureFig. 5).
289 | The concentration of organics increased from 17 μg m⁻³ in July to ~30 μg m⁻³ in

290 October, and then remained relatively stable across the whole of wintertime. The
291 concentration of organics reached a minimum in April ($17 \mu\text{g m}^{-3}$), and then rapidly
292 increased to $37 \mu\text{g m}^{-3}$ in June. Correspondingly, the contribution of organics to NR-PM₁
293 increased from ~40% in summer to above 50% during wintertime (FigureFig. 6). A
294 higher concentration of carbonaceous aerosol in winter, compared to the other three
295 seasons, was also observed in Beijing (Zhang et al., 2013a; Zhao et al., 2013). The
296 seasonal variation of organics is primarily driven by emissions from various sources and
297 secondary production. While the POA, particularly from coal combustion emissions, is
298 significantly elevated during wintertime, the photochemically processed SOA dominates
299 OA in summer (Sun et al., 2012; Sun et al., 2013b). In the present study, chloride showed
300 a similar seasonal variation to that of organics. The chloride concentration during
301 wintertime ($2.8\text{--}3.3 \mu\text{g m}^{-3}$) was approximately six times that ($0.5 \mu\text{g m}^{-3}$) in summer.
302 The contribution of chloride to NR-PM₁ showed a similar seasonal trend, with the lowest
303 contribution in summer (~1%) and the highest in winter (~5–6%) (FigureFig. 6). High
304 concentrations of chloride in winter are associated with enhanced coal combustion
305 emissions (Sun et al., 2013b), but also with low ambient temperature, which facilitates
306 the formation of particle-phase ammonium chloride. Also note that chloride showed a
307 twice as high concentration and contribution in June than the other two months in
308 summer because agricultural burning is also a large source of chloride (Viana et al., 2008;
309 Cheng et al., 2014).

310 The seasonal variation of sulfate is different from organics and chloride. The sulfate
311 concentration gradually decreased from $10.1 \mu\text{g m}^{-3}$ in August to $4.9 \mu\text{g m}^{-3}$ in
312 November, which was associated with a synchronous decrease in solar radiation and O₃
313 (FigureFig. 2). The contribution of sulfate to NR-PM₁ showed a corresponding decrease
314 from 19% to 10%. The sulfate concentration then increased to $8.3\text{--}8.8 \mu\text{g m}^{-3}$ in
315 December and January, likely due to a significant increase of precursor SO₂ associated
316 with an increased demand for domestic heating during the winter season, which can be
317 oxidized to form sulfate via either gas-phase oxidation or aqueous-phase processing (Xu
318 et al., 2014b). Sulfate showed the highest concentration in June ($13.5 \mu\text{g m}^{-3}$) due to
319 secondary production, but possibly the impact of biomass burning as well. Indeed, a
320 recent study in the YRD region also found a large enhancement of sulfate in biomass

321 burning plumes in summer (Zhang et al., 2015). Nitrate showed minor seasonal variation,
322 with the monthly average concentration ranging from 8 to 15 $\mu\text{g m}^{-3}$, except in June (23
323 $\mu\text{g m}^{-3}$). It is interesting that a higher concentration of nitrate was observed in summer
324 and spring than in winter. On average, nitrate accounted for $\sim 25\%$ of NR-PM₁ during
325 summertime, but decreased to $\sim 15\%$ during wintertime (Figure Fig. 6). Although high
326 temperatures in summer favor the dissociation of ammonium nitrate particles to gas-
327 phase ammonia and nitric acid, the correspondingly high RH and excess gaseous
328 ammonia facilitate the transformation of nitric acid to aqueous NH₄NO₃ particles (Meng
329 et al., 2011; Sun et al., 2012). The lowest concentration of nitrate during wintertime
330 might be primarily caused by the weak photochemical production associated with low
331 solar radiation and oxidants (e.g., O₃). In addition, the higher particle acidity in winter
332 (Liu, 2012) and lower mixing ratio of gaseous ammonia may also suppress the formation
333 of ammonium nitrate particles (Zhang et al., 2007). The seasonal variation of ammonium
334 is similar to that of sulfate and nitrate because ammonium primarily exists in the form of
335 NH₄NO₃ and (NH₄)₂SO₄.

336 3.3 Diurnal variations

337 As demonstrated in Figure Fig. 7, the diurnal cycles of organics during the four
338 seasons were overall similar, characterized by two pronounced peaks occurring at noon
339 and during the evening time. PMF analysis of OA suggested that the noon peak was
340 primarily caused by cooking emissions, while the evening peak was driven by different
341 primary emissions (e.g., cooking, traffic, and coal combustion emissions) among the
342 different seasons (Sun et al., 2012; Sun et al., 2013b). It should be noted that the noon
343 peaks in summer were more significant than those in fall and winter. Indeed, the cooking
344 emissions, determined by subtracting the background (10:00–11:00) from the noon peak
345 (12:00–13:00), were $\sim 1.5\text{--}2 \mu\text{g m}^{-3}$ from September to the following March, which were
346 lower than the $\sim 3.5 \mu\text{g m}^{-3}$ calculated for June and July. This seasonal trend agreed with
347 that of temperature, indicating that cooking emissions are temperature dependent,
348 probably because of increased cooking activity in hot summers than cold winters.

349 Relatively flat diurnal cycles were observed for sulfate during most months,
350 indicating the regional characteristics of sulfate. In fact, multi-day build-up of sulfate was

351 | frequently observed during all seasons (FigureFig. 3), supporting the notion of regional
352 | influences on sulfate in Beijing. It should be noted that the daytime photochemical
353 | production of sulfate from gas-phase oxidation of SO₂ might be masked by an elevated
354 | planetary boundary layer (PBL). Considering the dilution effect of the PBL, Sun et al.
355 | (2012) found that sulfate increased gradually from morning to late afternoon,
356 | demonstrating the daytime photochemical production of sulfate. In this study, sulfate in
357 | May, June and October showed an evident daytime increase until late afternoon,
358 | indicating an important role played by gas-phase photochemical processing in driving the
359 | sulfate diurnal cycle.

360 | Nitrate showed substantially different diurnal cycles among different months. A clear
361 | daytime increase starting from ~~about 8:00 to 19:00~~~~–08:00 until ~19:00~~ was found in the
362 | five months of January, February, March, November and December, indicating that such
363 | a diurnal pattern is more significant during wintertime compared to the fall and spring
364 | seasons. Figure 2 shows that the temperature during these five months was generally low
365 | (< 10°C), under which the partitioning of NH₄NO₃ into gaseous NH₃ and HNO₃ would
366 | not be significant. As a result, photochemical production would be the primary factor
367 | driving the diurnal variations. The photochemical production rate calculated from the
368 | daytime increase was 0.6–0.8 μg m⁻³ hr⁻¹ during winter and ~0.2–0.3 μg m⁻³ hr⁻¹ in
369 | November and March. Nitrate presented pronounced diurnal cycles in summer (June,
370 | July and August), with the concentrations gradually decreasing during daytime and
371 | reaching a minimum at ~16:00. Similar diurnal cycles have been observed on many
372 | occasions in summer in Beijing (Huang et al., 2010; Sun et al., 2012; Zhang et al., 2015).
373 | The evaporative loss of NH₄NO₃ associated with high temperatures, which overcomes the
374 | amount of photochemical production, plays the major role in driving such diurnal cycles.
375 | The rising PBL plays an additional role in the low concentrations of nitrate during
376 | daytime (Sun et al., 2012). The diurnal cycle of nitrate in May and September was also
377 | significant, characterized by a pronounced morning peak occurring at ~10:00, when
378 | photochemical production dominated over the gas–particle partitioning of NH₄NO₃.
379 | Nitrate showed a relatively flat diurnal cycle in April, indicating a combined effect of
380 | various nitrate formation mechanisms.

381 Chloride in this study was ~~mainly-primarily~~ detected as ammonium chloride because
382 ACSM is insensitive to refractory NaCl and/or KCl at its vaporizer temperature of 600°C;
383 ~~which shows similar volatile properties as NH₄NO₃~~. As shown in ~~FigureFig.~~ 7, two
384 different diurnal cycles were observed throughout different months. For the months of
385 July, August, September, April and May, chloride presented a morning peak when both
386 temperatures and the PBL were at their lowest, and then rapidly decreased to a low
387 ambient level at ~18:00. Such a diurnal cycle was likely primarily driven by temperature
388 dependent gas–particle partitioning (Hu et al., 2008). The diurnal cycles of chloride
389 during the remaining months were also significant, all of which were characterized by
390 high concentrations at night. Coincidentally, these months fell during the season of high
391 domestic-heating demand, which usually starts on 15 November and ends on 15 March.
392 Coal combustion has been found to be a large source of chloride (Zhang et al., 2012; Sun
393 et al., 2013b). Therefore, the diurnal cycle of chloride is likely dominantly driven by coal
394 combustion emissions that are intensified at night for domestic heating.

395 **3.4 Weekend effects**

396 Because the switch between clean periods and pollution episodes arising from
397 different source areas happens frequently in Beijing (Sun et al., 2013b; Guo et al., 2014),
398 the diurnal cycles of aerosol species can vary greatly due to the influences of different
399 occurrences of clean periods between weekdays and weekends (Sun et al., 2013b).
400 Therefore, periods with low aerosol loadings (NR-PM₁ < 20 μg m⁻³) were excluded from
401 the results (~~FigureFig.~~ 8) for a better investigation of the weekend effects (for the average
402 diurnal cycles with clean periods included, see ~~FigureFig.~~ S2S3). As shown in ~~FigureFig.~~
403 8, there were no clear weekend effects in the summer, except for slightly lower
404 concentrations of organics, sulfate and nitrate in the late afternoon at weekends. This
405 suggests that no significant differences in anthropogenic activity between weekdays and
406 weekends in summer. Although some enhanced traffic emissions between 00:00 and
407 06:00 at weekends might have occurred, as indicated by the higher concentration of NO
408 (~~FigureFig.~~ S3S4), they appeared to have negligible impacts on secondary sulfate and
409 nitrate. While the diurnal variations of organics and chloride were similar between
410 weekdays and weekends during the fall season, sulfate and nitrate showed pronounced
411 weekend effects, with persistently higher concentrations at weekends throughout the day.

412 An explanation for this is the stronger photochemical production of secondary species
413 associated with higher O₃ and solar radiation at weekends (Figure S3S4).
414 Consistently, SOA showed similar weekend effects as those of secondary inorganic
415 species, while POA did not (Sun et al., in preparation). Because of the regional
416 characteristics of secondary aerosols, further analysis is needed to address the impacts of
417 regional transport on the weekend effects of secondary species. Winter showed the most
418 pronounced weekend effects for all aerosol species. All aerosol species showed much
419 lower concentrations at weekends than on weekdays across the entire day, which was
420 consistent with those of NO, SO₂, and CO (Figure S3S4). These results clearly
421 indicate much reduced anthropogenic activity at weekends during wintertime because of
422 low ambient temperature (−4°C to −3°C). Further evidence is provided by the diurnal
423 cycles of organics, which presented pronounced noon peaks at weekends during all
424 seasons except winter. This observation was consistent with much reduced cooking
425 activity at weekends during wintertime. Similar to summer, no evident weekend effects
426 were observed in spring. The weekend effects of aerosol species in this study are overall
427 consistent with those observed by Han et al. (2009), in which similar diurnal cycles of
428 primary elemental carbon, CO, and CO₂ between weekdays and weekends under weak
429 wind conditions were observed during the three seasons other than winter.

430 3.5 Meteorological effects

431 Figure 9 shows the RH and *T* dependent distributions of NR-PM₁ and WS for the
432 entire year. The distribution of NR-PM₁ showed an obvious concentration gradient as a
433 function of RH. NR-PM₁ showed the lowest mass loading, generally less than 20 μg m^{−3}
434 at RH < 20%, and had no clear dependence on *T*. This can be explained by the high WS
435 (often larger than 5 m s^{−1}; Figure 9b) at low RH levels associated with clean air
436 masses from the north and/or northwest. Previous studies have also found a strong
437 association between low aerosol loading and high WS in Beijing (Han et al., 2009; Sun et
438 al., 2013b). NR-PM₁ showed moderately high concentrations (~20–40 μg m^{−3}) at low RH
439 (20–40%), which rapidly increased to a high concentration level (> 60 μg m^{−3}) at RH >
440 50%. These results indicate that severe haze episodes in Beijing mostly occur under high
441 humidity conditions, when WS is low as well. Two different regions with high
442 concentrations of NR-PM₁ are apparent in Figure 9a: one in the top-right region with

443 high temperature ($>15^{\circ}\text{C}$), and another in the bottom-right region with low ambient
444 temperature ($<6^{\circ}\text{C}$). Such a difference in distribution illustrates the severity of PM
445 pollution in different seasons. Note that low concentrations of NR-PM₁ sometimes
446 occurred at RH $> 90\%$, likely due to the scavenging of particles by rain or winter snow.

447 | The RH- and T -dependent distributions of major aerosol species (Figure 10) allow
448 us to further investigate the RH/ T impacts on the formation of aerosol species. While all
449 aerosol species showed similar concentration gradients as a function of RH to that of NR-
450 PM₁, the T -dependent patterns varied greatly. Organics generally showed the highest
451 concentrations under low T ($< 6^{\circ}\text{C}$) and high humidity conditions – very similar to the
452 behavior of chloride, which is mainly derived from combustion sources, e.g., coal
453 combustion or biomass burning (Zhang et al., 2012; Cheng et al., 2014). The results
454 suggest that high concentrations of organics during wintertime are primarily caused by
455 coal combustion emissions during the domestic-heating season, particularly from
456 residential coal combustion (Zhang et al., 2008). In fact, a previous study by our group
457 found that nearly one-third of OA during wintertime is primary coal combustion OA
458 (CCOA) (Sun et al., 2013b). In contrast, organics showed much lower concentrations
459 under the conditions of higher RH and higher T , for which one of the reasons was
460 probably far fewer coal combustion emissions during summertime (Zheng et al., 2005;
461 Zhang et al., 2013a). Consistently, CCOA has not yet been resolved from PMF analyses
462 of AMS OA in summer in Beijing (Huang et al., 2010; Sun et al., 2010). Note that the
463 region with a high concentration of organics corresponded to a high concentration of NR-
464 PM₁. In this region, organics accounted for the largest fraction of NR-PM₁
465 (approximately 40–50%), indicating that severe PM pollution under low temperature and
466 high humidity conditions is dominantly contributed to by organics. The mass fraction of
467 organics, however, showed an opposite distribution to that of mass loading. As shown in
468 | Figure 10, organics presents the highest contribution to NR-PM₁ ($\sim > 50\%$) in the
469 left-hand region with low RH, indicating the dominance of organics during periods with
470 low NR-PM₁ mass loadings. Such a distribution is independent of temperature,
471 suggesting a ubiquitously organics-dominant composition during clean days in all
472 seasons.

473 The RH/ T dependence of secondary inorganic species showed somewhat different
474 behaviors from that of organics. Sulfate presented two high concentration regions, with
475 the highest values occurring during wintertime when T was below 0°C and RH was
476 above 70%. Aqueous-phase oxidation, mostly fog processing, has been found to play a
477 dominant role in sulfate formation under such meteorological conditions (Sun et al.,
478 2013a). Surprisingly, the semi-volatile nitrate showed a relatively homogeneous
479 distribution across different temperatures at RH > 40%. Despite high temperature in
480 summer, high humidity facilitates the transformation of gaseous species into aqueous-
481 phase nitrate particles (Sun et al., 2012), particularly in the presence of high abundance of
482 gaseous ammonia (Ianniello et al., 2010). In fact, nitrate showed the highest contribution
483 (>~25%) to NR-PM₁ mass under high T and high RH conditions, which were also the
484 conditions under which high concentrations of NR-PM₁ were observed. The fact that
485 nitrate contributed more than sulfate (~15–20%) to NR-PM₁ mass during these conditions
486 suggests an important role played by nitrate in summer haze formation. While the
487 concentration of nitrate at various temperatures was close, its contribution to NR-PM₁
488 was generally lower at low temperatures due to the greater enhancement of organics
489 during wintertime. Also note that the two semi-volatile species, i.e., nitrate and chloride,
490 show the lowest contributions to NR-PM₁ in the top-left region with the highest T and
491 lowest RH. This illustrates the evaporative loss process of ammonium nitrate and
492 ammonium chloride under high temperatures in summertime. However, sulfate shows a
493 relatively higher contribution in this region since ammonium sulfate is less volatile than
494 ammonium nitrate and chloride (Huffman et al., 2009).

495 3.6 Source analysis

496 In summer, all NR-PM₁ species showed evident wind sector gradients, with higher
497 concentrations in association with winds from the east (E) and southeast (SE), and lower
498 concentrations with northwest (NW) wind (Figure Fig. 11). The average NR-PM₁
499 concentration from the SE was $89.5 \mu\text{g m}^{-3}$, which was more than twice that ($39.4 \mu\text{g}$
500 m^{-3}) from the NW. All aerosol species increased as wind sectors changed along the N–
501 NE–E–SE gradient, and then decreased along the SE–S–SW–W gradient. Such wind
502 sector dependence of aerosol composition is remarkably consistent with the spatial
503 distribution of fine particles in Beijing in 2013 (Beijing Environmental Statement 2013).

504 These results suggest an inhomogeneous distribution of air pollution around the IAP
505 sampling site in summer. Organics dominated NR-PM₁ across different sectors (37–
506 43%), followed by nitrate (21–28%), sulfate (15–20%), and ammonium (15–17%). While
507 chloride contributed a small fraction of NR-PM₁ (0.7–1.8%), the mass concentration
508 showed the largest difference between SE and NW. The fall season showed a similar
509 aerosol composition dependence as that in summer, with higher concentrations from the
510 E, SE, and S. However, the gradients of wind sectors appeared to be smaller. For
511 example, the average NR-PM₁ concentration ranged from 46.3 to 72.7 $\mu\text{g m}^{-3}$ in all eight
512 sectors except NW. Organics showed a similar dominance in NR-PM₁, accounting for
513 47–55%, and the contribution was ubiquitously higher than in summer for all wind
514 sectors. It should be noted that the NW sector showed the largest difference between
515 mean and median values for all species. The much lower median values suggest a
516 dominance of clean days for most of the time in this sector. In contrast, the summer
517 season showed higher median concentrations from the NW, indicating a higher regional
518 background during this season. The winter season showed consistently high
519 concentrations of PM across the different wind sectors, except for NW, where the mass
520 concentrations were approximately half of those in the other sectors. The average NR-
521 PM₁ ranged from 55.0 to 84.4 $\mu\text{g m}^{-3}$, with organics being the major fraction, accounting
522 for 46–54%. The spring season showed a similar wind sector dependence on aerosol
523 composition as the fall season. The average NR-PM₁ ranged from 49.0 to 74.4 $\mu\text{g m}^{-3}$ for
524 all of the wind sectors except the N (38.5 $\mu\text{g m}^{-3}$) and NW (24.7 $\mu\text{g m}^{-3}$), which had
525 much lower mass concentrations. Similar to other seasons, organics dominated NR-PM₁
526 throughout the different sectors (36–53%), followed by nitrate (19–27%) and sulfate (11–
527 16%).

528 | As ~~Figure~~Fig. 12 shows, the potential source areas for aerosol species varied among
529 the four seasons. In summer, high potential source areas were mainly located to the south,
530 southwest and southeast of Beijing. Organics had a relatively small high potential source
531 region in the south of Beijing (< 100 km) and a small source region located around
532 Baoding – one of the most polluted cities in Hebei Province. A narrow and visible source
533 area to the southeast of Beijing, including Tianjin and the Bohai Sea, was also observed.
534 Nitrate and chloride showed similar source areas to organics. The high potential source

535 area to the southeast Beijing was mainly caused by open agricultural burning in June in
536 northern China. Sulfate showed a distinct source region characterized by a narrow high
537 PSCF band along Hengshui–Baoding–Langfang–Beijing. Such a pollution band agrees
538 well with the topography of the North China Plain, with the Taihang Mountains to the
539 west and Yan Mountains to the north. The wide area of high PSCF for sulfate also
540 indicates a regional characteristic of sulfate that is formed from gas-phase oxidation or
541 cloud processing of precursor SO₂, which is particularly high in Hebei Province (Ji et al.,
542 2014). Secondary nitrate showed a similar, yet much smaller, PSCF region compared to
543 sulfate. One reason for this might be due to the evaporative loss of ammonium nitrate
544 during the long-range transport in summer.

545 All aerosol species showed similar PSCF spatial distributions during the fall season,
546 with high potential source regions located in a narrow area from Hengshui, Baoding to
547 Beijing. These results suggest that regional transport from the southwest plays a
548 dominant role in formation of severe haze pollution in fall. The wintertime results
549 showed largely different PSCF distributions from the other seasons. High PSCF values
550 were mainly located in a small region (< 50 km) in the south and southeast of Beijing.
551 Although Hebei Province often has worse air pollution than Beijing during wintertime (Ji
552 et al., 2014), the cities far away from Beijing appear not to be a very important source of
553 wintertime air pollution in Beijing. One explanation for this is that stagnant
554 meteorological conditions occur more frequently in winter due to low WS and *T*
555 inversions. Thus, local emissions and transport from nearby regions would play a more
556 significant role in affecting the pollution level in Beijing. While the spring season showed
557 similarly small high potential source regions to those during wintertime, an obvious high
558 potential source area in Hebei Province was also observed. The transport of air pollution
559 from the SW to the NE along the Taihang Mountains in northern China has been
560 observed many times in previous studies (Wang et al., 2014a; Wang et al., 2014c). Given
561 that many cities located on this pathway are often highly polluted, such as
562 Shijiazhuang, Baoding, and Hengshui, regional transport from these areas would have
563 a potentially high impact on the formation of severe haze pollution in Beijing.

564 **4 Conclusion**

565 This paper presents the results from a year-long, real-time measurement study of
566 submicron aerosol particle composition using an ACSM, conducted at an urban site in
567 Beijing from July 2011 to June 2012. The mass concentration of NR-PM₁ varied
568 dramatically, with the seasonal average concentration ranging from 52 to 62 μg m⁻³.
569 Organics comprised a major fraction of NR-PM₁ during all seasons, accounting for 40–
570 51% on average. The average contribution of nitrate to NR-PM₁ (17–25%) exceeded that
571 of sulfate (12–17%) during all seasons, suggesting an enhanced role of nitrate in PM
572 pollution in recent years. Organics and chloride were two species showing pronounced
573 seasonal variations in both mass concentrations and mass fractions. The higher
574 concentrations of organics and chloride in winter than summer were largely due to
575 enhanced coal combustion emissions. We also observed high concentrations of organics
576 and chloride in June and October – two months with strong agricultural burning impacts.
577 The seasonal variations of secondary sulfate and nitrate were not significant because of
578 the large variations of precursor concentrations, photochemical production, and also
579 meteorological effects in different seasons. However, higher contributions of SIA in
580 summer (57–61%) than in winter (43–46%) were still observed, indicating a more
581 significant role of secondary production in summer. The diurnal cycles of organics were
582 similar during all seasons, all characterized by two pronounced peaks. While the diurnal
583 cycles of secondary sulfate were overall relatively flat during most months of the year,
584 those of nitrate varied greatly in different seasons. It was evident that the diurnal cycles
585 of nitrate are driven by gas-particle partitioning and daytime photochemical production in
586 summer and winter, respectively. The winter season showed substantially different
587 concentrations of aerosol species between weekdays and weekends, with much lower
588 concentrations on weekends. However, no significant weekend effects were observed
589 during the other seasons.

590 | Meteorological conditions play important roles in the formation of severe PM
591 pollution in Beijing. In this study, we illustrate the influences of RH and *T* on aerosol
592 loading and chemistry in different seasons. All aerosol species increased significantly
593 under stagnant meteorological conditions associated with high RH and low WS. NR-
594 PM₁ showed two high concentration regions (> 60 μg m⁻³) at RH > 60%. While organics
595 comprised a major fraction of NR-PM₁ in these two regions, the abundances of sulfate

596 and nitrate and air temperature were largely different, suggesting they play different roles
597 in causing PM pollution during different seasons. Under drier conditions ($RH < 30\%$), the
598 NR-PM₁ concentration was generally low and organics contributed more than 50% of its
599 mass, indicating the importance of organics during clean periods. The semi-volatile
600 nitrate presented the largest contribution under high RH and high T , highlighting the
601 importance of nitrate formation via aqueous-phase processing in summer. All NR-PM₁
602 species showed obvious dependence on wind direction, with higher concentrations
603 commonly associated with winds from the S, E and SE. This was consistent with the
604 results from PSCF analysis, which showed that the high potential source areas were
605 mainly located to the S and SW of Beijing. The high potential source areas varied
606 differently during the four seasons. A common high potential source area to the SW of
607 Beijing, along the Taihang Mountains, was observed during all seasons except winter,
608 demonstrating the potentially high impact of regional transport on severe PM pollution in
609 Beijing. The winter season showed a much smaller source region compared to the other
610 seasons, indicating that local and regional transport over a smaller regional scale are more
611 important. High potential source areas to the SE of Beijing were also observed for
612 organics, nitrate and chloride in summer, likely due to agricultural burning.

613

614 **Acknowledgements**

615 This work was supported by the National Key Project of Basic Research
616 (2014CB447900; 2013CB955801), the Strategic Priority Research Program (B) of the
617 Chinese Academy of Sciences (XDB05020501), and the National Natural Science
618 Foundation of China (41175108).

619

620 **References**

621 Budisulistiorini, S. H., Canagaratna, M. R., Croteau, P. L., Marth, W. J., Baumann, K.,
622 Edgerton, E. S., Shaw, S., Knipping, E. M., Worsnop, D. R., and Jayne, J. T.: Real-
623 time continuous characterization of secondary organic aerosol derived from isoprene
624 epoxydiols (IEPOX) in downtown Atlanta, Georgia, using the Aerodyne Aerosol
625 Chemical Speciation Monitor (ACSM), *Environ. Sci. Technol.*, 47, 5686-5694, 2013.

626 Budisulistiorini, S. H., Canagaratna, M. R., Croteau, P. L., Baumann, K., Edgerton, E. S.,
627 Kollman, M. S., Ng, N. L., Verma, V., Shaw, S. L., Knipping, E. M., Worsnop, D. R.,
628 Jayne, J. T., Weber, R. J., and Surratt, J. D.: Intercomparison of an Aerosol Chemical
629 Speciation Monitor (ACSM) with ambient fine aerosol measurements in downtown
630 Atlanta, Georgia, *Atmos. Meas. Tech.*, 7, 1929-1941, 10.5194/amt-7-1929-2014,
631 2014.

632 Canagaratna, M., Jayne, J., Jimenez, J. L., Allan, J. A., Alfarra, R., Zhang, Q., Onasch,
633 T., Drewnick, F., Coe, H., Middlebrook, A., Delia, A., Williams, L., Trimborn, A.,
634 Northway, M., Kolb, C., Davidovits, P., and Worsnop, D.: Chemical and
635 microphysical characterization of aerosols via Aerosol Mass Spectrometry, *Mass
636 Spectrom. Rev.*, 26, 185-222, 2007.

637 Cao, J., Xu, H., Xu, Q., Chen, B., and Kan, H.: Fine particulate matter constituents and
638 cardiopulmonary mortality in a heavily polluted Chinese city, *Environ. Health
639 Perspect.*, 120, 373 - 378, 2012.

640 Carbone, S., Saarikoski, S., Frey, A., Reyes, F., Reyes, P., Castillo, M., Gramsch, E.,
641 Oyola, P., Jayne, J., and Worsnop, D. R.: Chemical characterization of submicron
642 aerosol particles in Santiago de Chile, *Aerosol Air Qual. Res.*, 13, 462-473, 2013.

643 Chen, Y., Sheng, G., Bi, X., Feng, Y., Mai, B., and Fu, J.: Emission factors for
644 carbonaceous particles and polycyclic aromatic hydrocarbons from residential coal
645 combustion in China, *Environ. Sci. Technol.*, 39, 1861-1867, 10.1021/es0493650,
646 2005.

647 Cheng, Y., Engling, G., He, K.-B., Duan, F.-K., Du, Z.-Y., Ma, Y.-L., Liang, L.-L., Lu,
648 Z.-F., Liu, J.-M., Zheng, M., and Weber, R. J.: The characteristics of Beijing aerosol
649 during two distinct episodes: Impacts of biomass burning and fireworks, *Environ.
650 Pollut.*, 185, 149-157, <http://dx.doi.org/10.1016/j.envpol.2013.10.037>, 2014.

651 DeCarlo, P. F., Kimmel, J. R., Trimborn, A., Northway, M. J., Jayne, J. T., Aiken, A. C.,
652 Gonin, M., Fuhrer, K., Horvath, T., Docherty, K. S., Worsnop, D. R., and Jimenez, J.
653 L.: Field-Deployable, High-Resolution, Time-of-Flight Aerosol Mass Spectrometer,
654 *Anal. Chem.*, 78, 8281-8289, 2006.

655 Docherty, K. S., Aiken, A. C., Huffman, J. A., Ulbrich, I. M., DeCarlo, P. F., Sueper, D.,
656 Worsnop, D. R., Snyder, D. C., Peltier, R. E., Weber, R. J., Grover, B. D., Eatough,
657 D. J., Williams, B. J., Goldstein, A. H., Ziemann, P. J., and Jimenez, J. L.: The 2005
658 Study of Organic Aerosols at Riverside (SOAR-1): instrumental intercomparisons
659 and fine particle composition, *Atmos. Chem. Phys.*, 11, 12387-12420, 10.5194/acp-
660 11-12387-2011, 2011.

661 Draxler, R. R., and Rolph, G. D.: HYSPLIT (HYbrid Single-Particle Lagrangian
662 Integrated Trajectory) Model access via NOAA ARL READY Website
663 (<http://www.arl.noaa.gov/ready/hysplit4.html>), NOAA Air Resources Laboratory,
664 Silver Spring, MD., 2003.

665 Drewnick, F., Hings, S. S., DeCarlo, P. F., Jayne, J. T., Gonin, M., Fuhrer, K., Weimer,
666 S., Jimenez, J. L., Demerjian, K. L., Borrmann, S., and Worsnop, D. R.: A new Time-
667 of-Flight Aerosol Mass Spectrometer (ToF-AMS) – Instrument description and first
668 field deployment., *Aerosol Sci. Tech.*, 39, 637-658, 2005.

669 Gong, Z., Lan, Z., Xue, L., Zeng, L., He, L., and Huang, X.: Characterization of
670 submicron aerosols in the urban outflow of the central Pearl River Delta region of
671 China, *Front. Environ. Sci. Eng.*, 6, 725-733, 10.1007/s11783-012-0441-8, 2012.

672 Guo, S., Hu, M., Zamora, M. L., Peng, J., Shang, D., Zheng, J., Du, Z., Wu, Z., Shao, M.,
673 Zeng, L., Molina, M. J., and Zhang, R.: Elucidating severe urban haze formation in
674 China, *Proc. Natl. Acad. Sci. U.S.A.*, 111, 17373-17378, 10.1073/pnas.1419604111,
675 2014.

676 Han, S., Kondo, Y., Oshima, N., Takegawa, N., Miyazaki, Y., Hu, M., Lin, P., Deng, Z.,
677 Zhao, Y., Sugimoto, N., and Wu, Y.: Temporal variations of elemental carbon in
678 Beijing, *J. Geophys. Res.*, 114, D23202, doi:23210.21029/22009JD012027, 2009.

679 He, L.-Y., Huang, X.-F., Xue, L., Hu, M., Lin, Y., Zheng, J., Zhang, R., and Zhang, Y.-
680 H.: Submicron aerosol analysis and organic source apportionment in an urban
681 atmosphere in Pearl River Delta of China using high-resolution aerosol mass
682 spectrometry, *J. Geophys. Res.*, 116, D12304, 10.1029/2010jd014566, 2011.

683 Hu, M., Wu, Z., Slanina, J., Lin, P., Liu, S., and Zeng, L.: Acidic gases, ammonia and
684 water-soluble ions in PM_{2.5} at a coastal site in the Pearl River Delta, China, *Atmos.*
685 *Environ.*, 42, 6310-6320, 10.1016/j.atmosenv.2008.02.015, 2008.

686 Hu, W. W., Hu, M., Yuan, B., Jimenez, J. L., Tang, Q., Peng, J. F., Hu, W., Shao, M.,
687 Wang, M., Zeng, L. M., Wu, Y. S., Gong, Z. H., Huang, X. F., and He, L. Y.: Insights
688 on organic aerosol aging and the influence of coal combustion at a regional receptor
689 site of central eastern China, *Atmos. Chem. Phys.*, 13, 10095-10112, 10.5194/acp-13-
690 10095-2013, 2013.

691 Huang, R.-J., Zhang, Y., Bozzetti, C., Ho, K.-F., Cao, J.-J., Han, Y., Daellenbach, K. R.,
692 Slowik, J. G., Platt, S. M., Canonaco, F., Zotter, P., Wolf, R., Pieber, S. M., Bruns, E.
693 A., Crippa, M., Ciarelli, G., Piazzalunga, A., Schwikowski, M., Abbaszade, G.,
694 Schnelle-Kreis, J., Zimmermann, R., An, Z., Szidat, S., Baltensperger, U., Haddad, I.
695 E., and Prevot, A. S. H.: High secondary aerosol contribution to particulate pollution
696 during haze events in China, *Nature*, 514, 218 - 222, 10.1038/nature13774, 2014.

697 Huang, X.-F., Xue, L., Tian, X.-D., Shao, W.-W., Sun, T.-L., Gong, Z.-H., Ju, W.-W.,
698 Jiang, B., Hu, M., and He, L.-Y.: Highly time-resolved carbonaceous aerosol
699 characterization in Yangtze River Delta of China: composition, mixing state and
700 secondary formation, *Atmos. Environ.*, 64, 200 - 207,
701 10.1016/j.atmosenv.2012.09.059, 2013.

702 Huang, X. F., He, L. Y., Hu, M., Canagaratna, M. R., Sun, Y., Zhang, Q., Zhu, T., Xue,
703 L., Zeng, L. W., Liu, X. G., Zhang, Y. H., Jayne, J. T., Ng, N. L., and Worsnop, D.
704 R.: Highly time-resolved chemical characterization of atmospheric submicron
705 particles during 2008 Beijing Olympic Games using an Aerodyne High-Resolution
706 Aerosol Mass Spectrometer, *Atmos. Chem. Phys.*, 10, 8933-8945, 10.5194/acp-10-
707 8933-2010, 2010.

708 Huang, X. F., He, L. Y., Hu, M., Canagaratna, M. R., Kroll, J. H., Ng, N. L., Zhang, Y.
709 H., Lin, Y., Xue, L., Sun, T. L., Liu, X. G., Shao, M., Jayne, J. T., and Worsnop, D.
710 R.: Characterization of submicron aerosols at a rural site in Pearl River Delta of
711 China using an Aerodyne High-Resolution Aerosol Mass Spectrometer, *Atmos.*
712 *Chem. Phys.*, 11, 1865-1877, 10.5194/acp-11-1865-2011, 2011.

713 Huang, X. F., He, L. Y., Xue, L., Sun, T. L., Zeng, L. W., Gong, Z. H., Hu, M., and Zhu,
714 T.: Highly time-resolved chemical characterization of atmospheric fine particles
715 during 2010 Shanghai World Expo, *Atmos. Chem. Phys.*, 12, 4897-4907,
716 10.5194/acp-12-4897-2012, 2012.

717 Huffman, J. A., Jayne, J. T., Drewnick, F., Aiken, A. C., Onasch, T., Worsnop, D. R., and
718 Jimenez, J. L.: Design, modeling, optimization, and experimental tests of a particle
719 beam width probe for the Aerodyne Aerosol Mass Spectrometer, *Aerosol Sci. Tech.*,
720 39, 1143-1163, 2005.

721 Huffman, J. A., Docherty, K. S., Aiken, A. C., Cubison, M. J., Ulbrich, I. M., DeCarlo, P.
722 F., Sueper, D., Jayne, J. T., Worsnop, D. R., Ziemann, P. J., and Jimenez, J. L.:
723 Chemically-resolved aerosol volatility measurements from two megacity field
724 studies, *Atmos. Chem. Phys.*, 9, 7161-7182, 2009.

725 Ianniello, A., Spataro, F., Esposito, G., Allegrini, I., Rantica, E., Ancora, M. P., Hu, M.,
726 and Zhu, T.: Occurrence of gas phase ammonia in the area of Beijing (China), *Atmos.*
727 *Chem. Phys.*, 10, 9487-9503, 10.5194/acp-10-9487-2010, 2010.

728 Jayne, J. T., Leard, D. C., Zhang, X., Davidovits, P., Smith, K. A., Kolb, C. E., and
729 Worsnop, D. R.: Development of an aerosol mass spectrometer for size and
730 composition analysis of submicron particles, *Aerosol Sci. Tech.*, 33, 49-70, 2000.

731 Ji, D., Li, L., Wang, Y., Zhang, J., Cheng, M., Sun, Y., Liu, Z., Wang, L., Tang, G., Hu,
732 B., Chao, N., Wen, T., and Miao, H.: The heaviest particulate air-pollution episodes
733 occurred in northern China in January, 2013: Insights gained from observation,
734 *Atmos. Environ.*, 92, 546-556, <http://dx.doi.org/10.1016/j.atmosenv.2014.04.048>,
735 2014.

736 Liu, Q.: Physical and chemical characteristics of submicron aerosol and its sources in
737 Beijing, LAPC, Institute of Atmospheric Physics, Chinese Academy of Sciences,
738 2012.

739 Matthew, B. M., Middlebrook, A. M., and Onasch, T. B.: Collection efficiencies in an
740 Aerodyne Aerosol Mass Spectrometer as a function of particle phase for laboratory
741 generated aerosols, *Aerosol Sci. Tech.*, 42, 884 - 898, 2008.

742 Meng, Z. Y., Lin, W. L., Jiang, X. M., Yan, P., Wang, Y., Zhang, Y. M., Jia, X. F., and
743 Yu, X. L.: Characteristics of atmospheric ammonia over Beijing, China, *Atmos.*
744 *Chem. Phys.*, 11, 6139-6151, 10.5194/acp-11-6139-2011, 2011.

745 Middlebrook, A. M., Bahreini, R., Jimenez, J. L., and Canagaratna, M. R.: Evaluation of
746 composition-dependent collection efficiencies for the Aerodyne Aerosol Mass
747 Spectrometer using field data, *Aerosol Sci. Tech.*, 46, 258-271, 2012.

748 Ng, N. L., Herndon, S. C., Trimborn, A., Canagaratna, M. R., Croteau, P. L., Onasch, T.
749 B., Sueper, D., Worsnop, D. R., Zhang, Q., Sun, Y. L., and Jayne, J. T.: An Aerosol
750 Chemical Speciation Monitor (ACSM) for routine monitoring of the composition and
751 mass concentrations of ambient aerosol, *Aerosol Sci. Tech.*, 45, 770 - 784, 2011.

752 Parworth, C., Fast, J., Mei, F., Shippert, T., Sivaraman, C., Tilp, A., Watson, T., and
753 Zhang, Q.: Long-term Measurements of Submicrometer Aerosol Chemistry at the
754 Southern Great Plains (SGP) Using an Aerosol Chemical Speciation Monitor
755 (ACSM), *Atmos. Environ.*, 106, 43-55,
756 <http://dx.doi.org/10.1016/j.atmosenv.2015.01.060>, 2015.

757 Petit, J. E., Favez, O., Sciare, J., Crenn, V., Sarda-Estève, R., Bonnaire, N., Močnik, G.,
758 Dupont, J. C., Haeffelin, M., and Leoz-Garziandia, E.: Two years of near real-time
759 chemical composition of submicron aerosols in the region of Paris using an Aerosol
760 Chemical Speciation Monitor (ACSM) and a multi-wavelength Aethalometer, *Atmos.*
761 *Chem. Phys.*, 15, 2985-3005, 10.5194/acp-15-2985-2015, 2015.

762 Polissar, A. V., P.K. Hopke, P. Paatero, Y.J. Kaufman, D.K. Hall, B.A. Bodhaine, E.G.
763 Dutton, J.M. Harris: The aerosol at Barrow, Alaska: long-term trends and source
764 locations, *Atmos. Environ.*, 33, 2441-2458, 1999.

765 Sun, J., Zhang, Q., Canagaratna, M. R., Zhang, Y., Ng, N. L., Sun, Y., Jayne, J. T.,
766 Zhang, X., Zhang, X., and Worsnop, D. R.: Highly time- and size-resolved
767 characterization of submicron aerosol particles in Beijing using an Aerodyne Aerosol
768 Mass Spectrometer, *Atmos. Environ.*, 44, 131-140, 2010.

769 Sun, Y. L., Wang, Z., Dong, H., Yang, T., Li, J., Pan, X., Chen, P., and Jayne, J. T.:
770 Characterization of summer organic and inorganic aerosols in Beijing, China with an
771 Aerosol Chemical Speciation Monitor, *Atmos. Environ.*, 51, 250-259,
772 [10.1016/j.atmosenv.2012.01.013](https://doi.org/10.1016/j.atmosenv.2012.01.013), 2012.

773 Sun, Y. L., Wang, Z., Fu, P., Jiang, Q., Yang, T., Li, J., and Ge, X.: The impact of
774 relative humidity on aerosol composition and evolution processes during wintertime
775 in Beijing, China, *Atmos. Environ.*, 77, 927–934,
776 <http://dx.doi.org/10.1016/j.atmosenv.2013.06.019>, 2013a.

777 Sun, Y. L., Wang, Z. F., Fu, P. Q., Yang, T., Jiang, Q., Dong, H. B., Li, J., and Jia, J. J.:
778 Aerosol composition, sources and processes during wintertime in Beijing, China,
779 *Atmos. Chem. Phys.*, 13, 4577-4592, [10.5194/acp-13-4577-2013](https://doi.org/10.5194/acp-13-4577-2013), 2013b.

780 Sun, Y. L., Jiang, Q., Wang, Z., Fu, P., Li, J., Yang, T., and Yin, Y.: Investigation of the
781 sources and evolution processes of severe haze pollution in Beijing in January 2013,
782 *J. Geophys. Res.*, 119, 4380-4398, [10.1002/2014JD021641](https://doi.org/10.1002/2014JD021641), 2014.

783 Viana, M., López, J. M., Querol, X., Alastuey, A., García-Gacio, D., Blanco-Heras, G.,
784 López-Mahía, P., Piñeiro-Iglesias, M., Sanz, M. J., Sanz, F., Chi, X., and Maenhaut,
785 W.: Tracers and impact of open burning of rice straw residues on PM in Eastern
786 Spain, *Atmos. Environ.*, 42, 1941-1957,
787 <http://dx.doi.org/10.1016/j.atmosenv.2007.11.012>, 2008.

788 Wang, L. T., Wei, Z., Yang, J., Zhang, Y., Zhang, F. F., Su, J., Meng, C. C., and Zhang,
789 Q.: The 2013 severe haze over southern Hebei, China: model evaluation, source
790 apportionment, and policy implications, *Atmos. Chem. Phys.*, 14, 3151-3173,
791 [10.5194/acp-14-3151-2014](https://doi.org/10.5194/acp-14-3151-2014), 2014a.

792 Wang, S. X., Zhao, B., Cai, S. Y., Klimont, Z., Nielsen, C. P., Morikawa, T., Woo, J. H.,
793 Kim, Y., Fu, X., Xu, J. Y., Hao, J. M., and He, K. B.: Emission trends and mitigation
794 options for air pollutants in East Asia, *Atmos. Chem. Phys.*, 14, 6571-6603,
795 [10.5194/acp-14-6571-2014](https://doi.org/10.5194/acp-14-6571-2014), 2014b.

796 Wang, Y., Zhang, Q. Q., He, K., Zhang, Q., and Chai, L.: Sulfate-nitrate-ammonium
797 aerosols over China: response to 2000–2015 emission changes of sulfur dioxide,
798 nitrogen oxides, and ammonia, *Atmos. Chem. Phys.*, 13, 2635-2652, [10.5194/acp-13-2635-2013](https://doi.org/10.5194/acp-13-2635-2013), 2013.

800 Wang, Z., Li, J., Wang, Z., Yang, W., Tang, X., Ge, B., Yan, P., Zhu, L., Chen, X., Chen,
801 H., Wang, W., Li, J., Liu, B., Wang, X., Wand, W., Zhao, Y., Lu, N., and Su, D.:
802 Modeling study of regional severe hazes over mid-eastern China in January 2013 and
803 its implications on pollution prevention and control, *Sci. China Earth Sci.*, 57, 3-13,
804 [10.1007/s11430-013-4793-0](https://doi.org/10.1007/s11430-013-4793-0), 2014c.

805 Xu, J., Zhang, Q., Chen, M., Ge, X., Ren, J., and Qin, D.: Chemical composition, sources,
806 and processes of urban aerosols during summertime in northwest China: insights from

807 high-resolution aerosol mass spectrometry, *Atmos. Chem. Phys.*, 14, 12593-12611,
808 10.5194/acp-14-12593-2014, 2014a.

809 Xu, W. Y., Zhao, C. S., Ran, L., Lin, W. L., Yan, P., and Xu, X. B.: SO₂ noontime-peak
810 phenomenon in the North China Plain, *Atmos. Chem. Phys.*, 14, 7757-7768,
811 10.5194/acp-14-7757-2014, 2014b.

812 Yang, F., Huang, L., Duan, F., Zhang, W., He, K., Ma, Y., Brook, J. R., Tan, J., Zhao, Q.,
813 and Cheng, Y.: Carbonaceous species in PM_{2.5} at a pair of rural/urban sites in Beijing,
814 2005–2008, *Atmos. Chem. Phys.*, 11, 7893-7903, 10.5194/acp-11-7893-2011, 2011.

815 Zhang, H., Wang, S., Hao, J., Wan, L., Jiang, J., Zhang, M., Mestl, H. E. S., Alnes, L. W.
816 H., Aunan, K., and Mellouki, A. W.: Chemical and size characterization of particles
817 emitted from the burning of coal and wood in rural households in Guizhou, China,
818 *Atmos. Environ.*, 51, 94-99, 10.1016/j.atmosenv.2012.01.042, 2012.

819 Zhang, Q., Jimenez, J. L., Worsnop, D. R., and Canagaratna, M.: A case study of urban
820 particle acidity and its effect on secondary organic aerosol, *Environ. Sci. Technol.*,
821 41, 3213-3219, 2007.

822 Zhang, R., Jing, J., Tao, J., Hsu, S. C., Wang, G., Cao, J., Lee, C. S. L., Zhu, L., Chen, Z.,
823 Zhao, Y., and Shen, Z.: Chemical characterization and source apportionment of PM_{2.5}
824 in Beijing: seasonal perspective, *Atmos. Chem. Phys.*, 13, 7053-7074, 10.5194/acp-
825 13-7053-2013, 2013a.

826 Zhang, Y., Schauer, J. J., Zhang, Y., Zeng, L., Wei, Y., Liu, Y., and Shao, M.:
827 Characteristics of particulate carbon emissions from real-world Chinese coal
828 combustion, *Environ. Sci. Technol.*, 42, 5068-5073, 2008.

829 Zhang, Y., Sun, J., Zhang, X., Shen, X., Wang, T., and Qin, M.: Seasonal
830 characterization of components and size distributions for submicron aerosols in
831 Beijing, *Sci. China Earth Sci.*, 56, 890 - 900, 10.1007/s11430-012-4515-z, 2013b.

832 Zhang, Y. J., Tang, L. L., Wang, Z., Yu, H. X., Sun, Y. L., Liu, D., Qin, W., Canonaco,
833 F., Prévôt, A. S. H., Zhang, H. L., and Zhou, H. C.: Insights into characteristics,
834 sources, and evolution of submicron aerosols during harvest seasons in the Yangtze
835 River delta region, China, *Atmos. Chem. Phys.*, 15, 1331-1349, 10.5194/acp-15-
836 1331-2015, 2015.

837 Zhao, P. S., Dong, F., He, D., Zhao, X. J., Zhang, X. L., Zhang, W. Z., Yao, Q., and Liu,
838 H. Y.: Characteristics of concentrations and chemical compositions for PM_{2.5} in the
839 region of Beijing, Tianjin, and Hebei, China, *Atmos. Chem. Phys.*, 13, 4631-4644,
840 10.5194/acp-13-4631-2013, 2013.

841 Zhao, X., Zhang, X., Xu, X., Xu, J., Meng, W., and Pu, W.: Seasonal and diurnal
842 variations of ambient PM_{2.5} concentration in urban and rural environments in Beijing,
843 *Atmos. Environ.*, 43, 2893-2900, 2009.

844 Zheng, G. J., Duan, F. K., Su, H., Ma, Y. L., Cheng, Y., Zheng, B., Zhang, Q., Huang, T.,
845 Kimoto, T., Chang, D., Pöschl, U., Cheng, Y. F., and He, K. B.: Exploring the severe
846 winter haze in Beijing: the impact of synoptic weather, regional transport and
847 heterogeneous reactions, *Atmos. Chem. Phys.*, 15, 2969-2983, 10.5194/acp-15-2969-
848 2015, 2015.

849 Zheng, M., Salmon, L. G., Schauer, J. J., Zeng, L., Kiang, C. S., Zhang, Y., and Cass, G.
850 R.: Seasonal trends in PM_{2.5} source contributions in Beijing, China, *Atmos. Environ.*,
851 39, 3967-3976, DOI: 10.1016/j.atmosenv.2005.03.036, 2005.

852

853 **Tables**

854 **Table 1.** Summary of mass concentrations of NR-PM₁ species, gaseous pollutants and
 855 meteorological parameters during the four seasons and entire study period.

	Entire study		Summer		Fall		Winter		Spring	
	mean	s.d.	mean	s.d.	mean	s.d.	mean	s.d.	mean	s.d.
Org ($\mu\text{g m}^{-3}$)	25.7	22.1	24.5	20.7	26.8	24.7	29.6	24.8	21.7	16.0
SO ₄ ²⁻ ($\mu\text{g m}^{-3}$)	8.1	8.3	10.6	8.2	6.5	7.5	7.7	9.2	7.3	7.6
NO ₃ ⁻ ($\mu\text{g m}^{-3}$)	12.6	12.8	15.6	14.4	11.4	12.7	10.3	9.5	13.1	13.4
NH ₄ ⁺ ($\mu\text{g m}^{-3}$)	8.5	7.9	10.2	8.2	6.9	7.3	8.1	7.4	8.8	8.1
Cl ⁻ ($\mu\text{g m}^{-3}$)	1.8	2.5	0.8	1.5	1.7	2.7	3.0	3.0	1.5	1.9
NR-PM ₁ ($\mu\text{g m}^{-3}$)	56.6	48.2	61.6	48.8	53.3	49.7	58.7	50.5	52.3	42.7
SO ₂ (ppb)	16.2	14.0	5.4	0.8			25.3	16.0	11.5	8.3
CO (ppm)	1.5	1.3	1.8	1.3			1.7	1.6	1.2	1.0
NO (ppb)	30.0	43.0	7.8	10.8	41.9	51.2	50.9	50.9	19.8	30.0
NO _y (ppb)	64.0	55.5	35.6	17.9	77.8	63.1	89.1	66.6	54.0	43.3
O ₃ (ppb)	21.2	23.8	33.3	29.1	20.3	24.4	7.9	8.5	20.8	19.3
RH (%)	47.0	23.4	62.7	18.9	52.7	20.0	35.6	20.3	36.5	22.5
T (°C)	13.3	11.6	26.3	3.6	14.1	7.0	-1.3	3.4	14.6	8.4
WS, 8 m	1.2	0.8	1.0	0.5	0.9	0.7	1.4	1.0	1.4	0.9
WS, 240 m	4.4	3.0	3.5	2.3	4.1	2.7	4.6	3.4	5.3	3.3

856

857 **Figure captions:**

858 | **FigureFig.** 1. (a) Map of the sampling site (IAP). (b) Wind rose plots, color coded by
859 | wind speed for each season. The frequencies are set to the same scales for all seasons.

860 | **FigureFig.** 2. Monthly variation of (a) gaseous O₃ and NO_y, (b) precipitation (Precip.) and
861 | solar radiation (SR), (c) wind speed (WS) and pressure (*P*), and (d) relative humidity
862 | (RH) and temperature (*T*). The WS at the heights of 8 m (solid gray circles) and 240 m
863 | (solid black circles) are shown in (c).

864 | **FigureFig.** 3. Time series of NR-PM₁ species for the entire year. The pie charts show the
865 | average chemical composition of NR-PM₁ during the four seasons (summer, fall, winter
866 | and spring).

867 | **FigureFig.** 4. Frequency of NR-PM₁ mass loadings during the four seasons: (a) summer;
868 | (b) fall; (c) winter; (d) spring. **Note that the frequency was calculated with 15 min**
869 | **average data.**

870 | **FigureFig.** 5. Seasonal variation of non-refractory submicron aerosol species. The bars
871 | represent the 25th and 75th percentiles.

872 | **FigureFig.** 6. Monthly variation of (a) mass concentrations and (b) mass fractions of NR-
873 | PM₁ species.

874 | **FigureFig.** 7. Monthly average diurnal cycle of (a) organics, (b) sulfate, (c) nitrate, and
875 | (d) chloride during the four seasons.

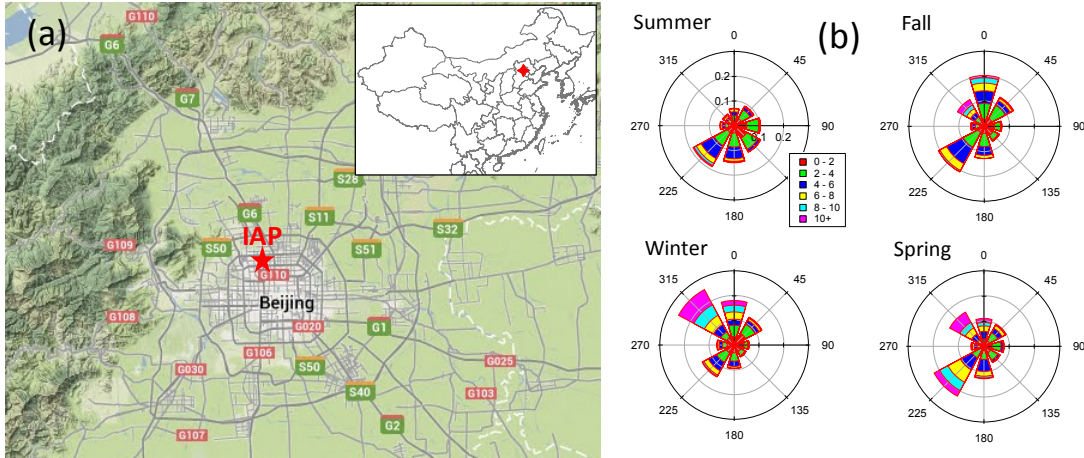
876 | **FigureFig.** 8. Comparison of the average diurnal cycles of (a) organics, (b) SO₄²⁻, (c)
877 | NO₃⁻, and (d) Cl⁻ between weekdays and weekends during the four seasons. Note that the
878 | periods with NR-PM₁ < 20 μg m⁻³ are excluded.

879 | **FigureFig.** 9. RH/*T* dependence of (a) NR-PM₁ mass concentration and (b) WS for a
880 | whole year. The data are grouped into grids with increments of RH and *T* being 5% and
881 | 3°C, respectively. Grids with the number of data points fewer than 10 are excluded.

882 | **FigureFig.** 10. RH/*T* dependence of mass concentrations and mass fractions of aerosol
883 | species for a whole year: (a) organics; (b) sulfate; (c) nitrate; (d) chloride. The data are
884 | grouped into grids with increments of RH and *T* being 5% and 3°C, respectively. Grids
885 | with the number of data points fewer than 10 are excluded.

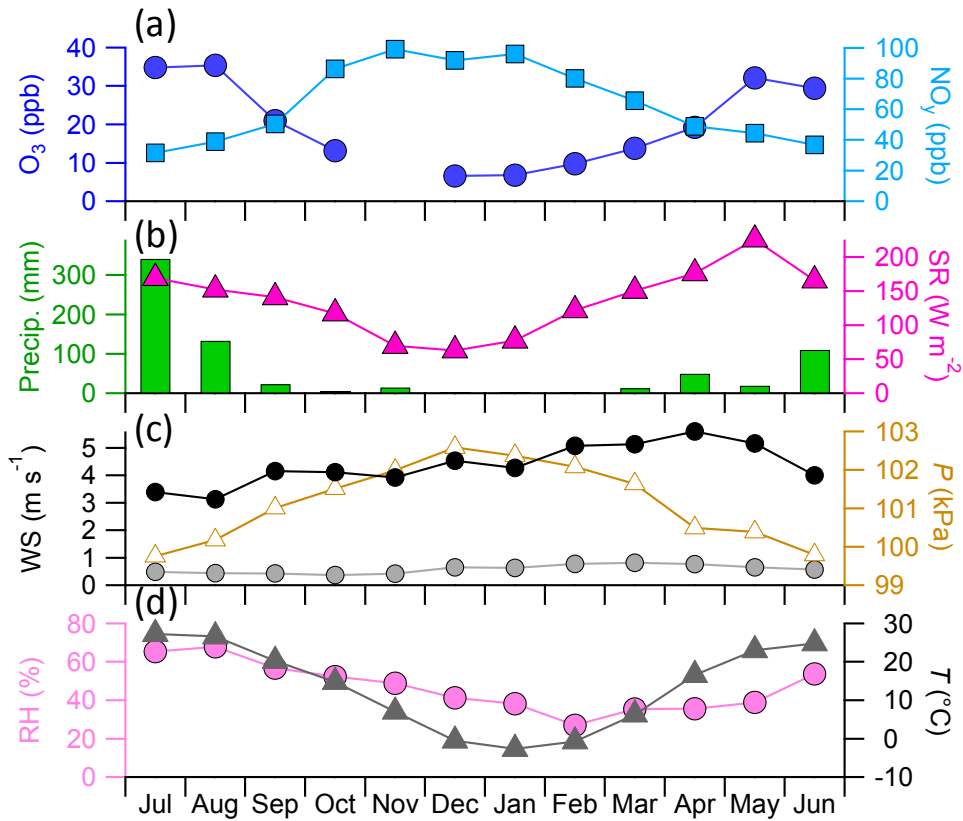
886 | **FigureFig.** 11. Box plots of mass concentrations of (a) organics, (b) SO₄²⁻, (c) NO₃⁻, and
887 | (d) Cl⁻ as a function of wind directions sectors. All the data were segregated into eight
888 | wind sectors representing north (N), northeast (NE), east (E), southeast (SE), south (S),
889 | southwest (SW), west (W), and northwest (NW). The mean (cross), median (horizontal
890 | line), 25th and 75th percentiles (lower and upper box), and 10th and 90th percentiles
891 | (lower and upper whiskers) are shown.

892 | **FigureFig.** 12. PSCF of NR-PM₁ species during four seasons: (a) organics; (b) sulfate; (c)
893 | nitrate; (d) chloride. The cities marked in each panel are Beijing (BJ), Tianjing (TJ),
894 | Langfang (LF), Baoding (BD), Shijiazhuang (SJZ), and Hengshui (HS). The color scales
895 | indicate the values of PSCF.



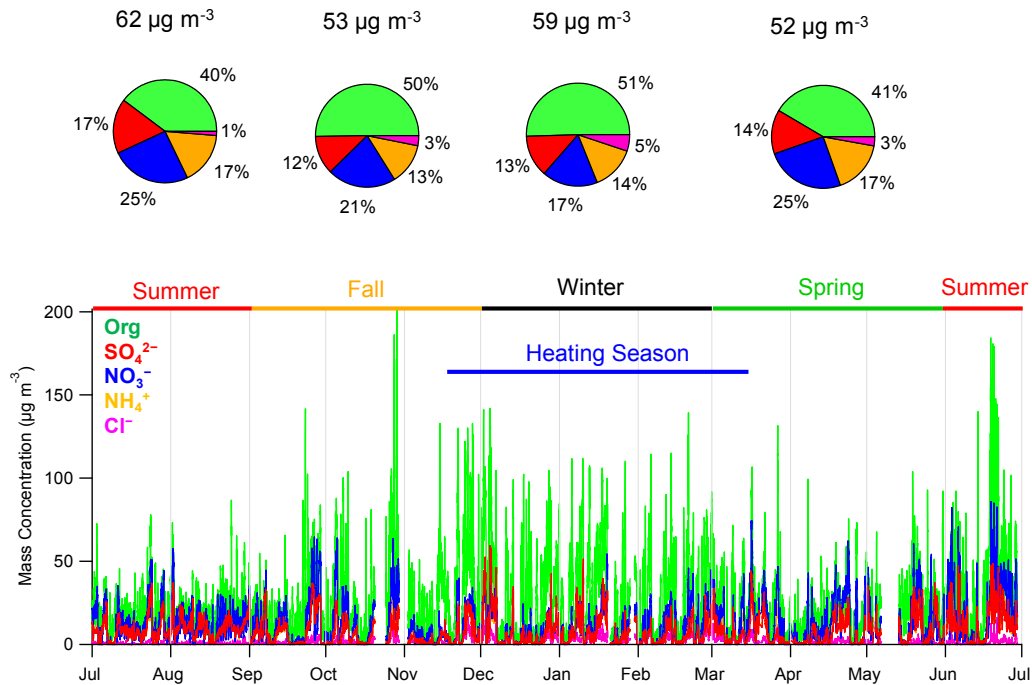
896

897 | **Figure** Fig. 1. (a) Map of the sampling site (IAP). (b) Wind rose plots, color coded by
 898 wind speed for each season. The frequencies are set to the same scales for all seasons.

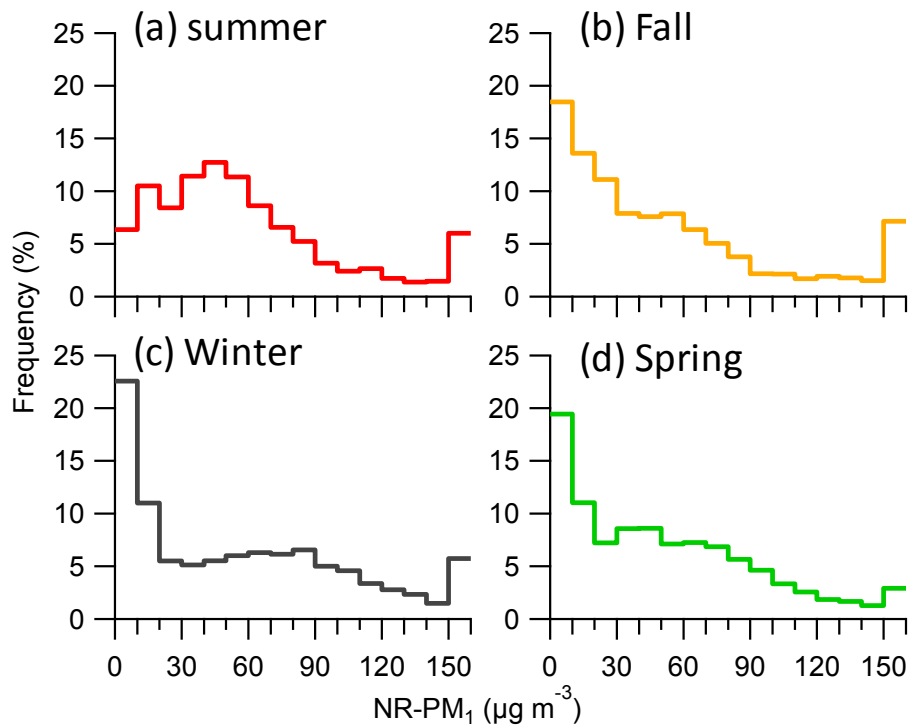


899

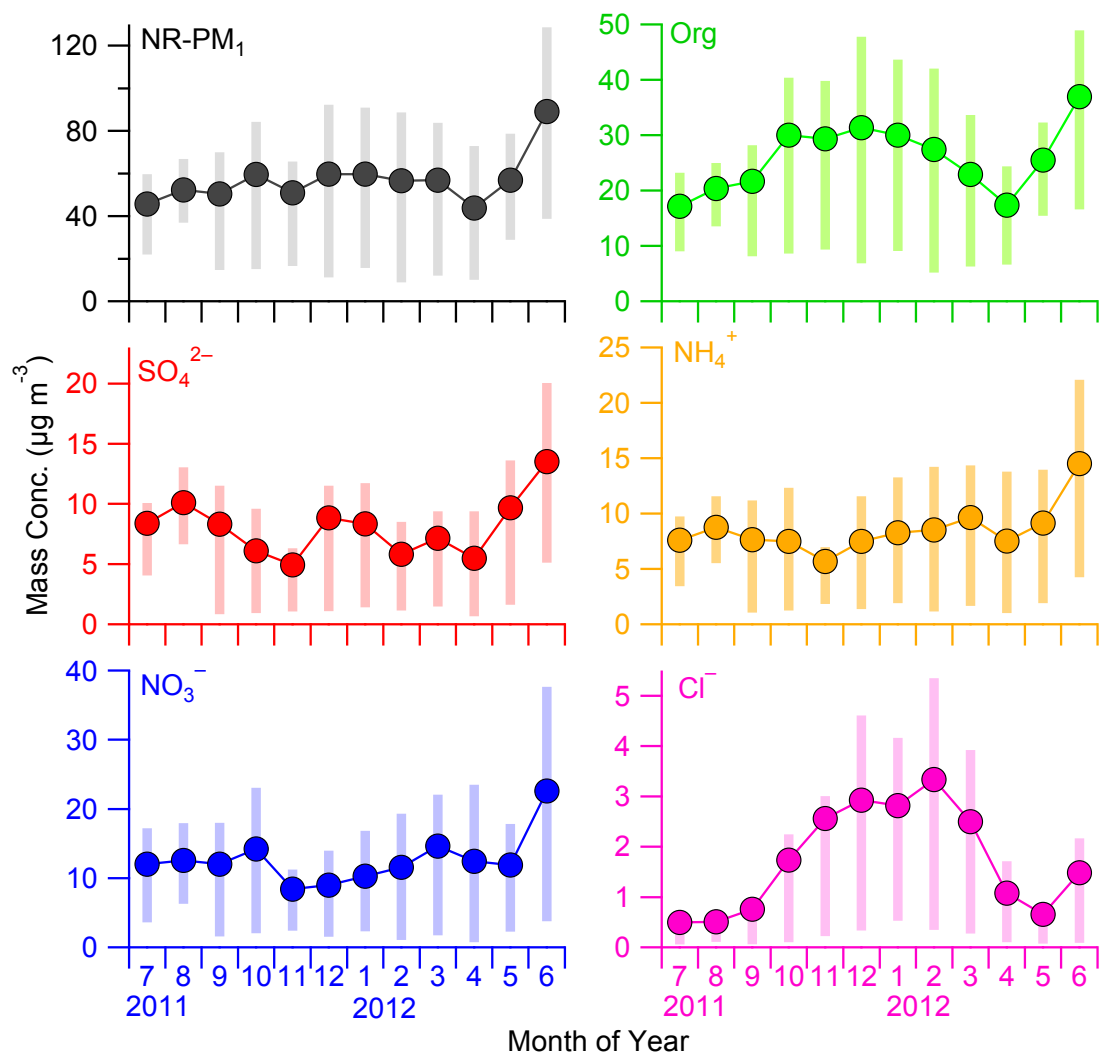
900 | **Figure** Fig. 2. Monthly variation of (a) gaseous O₃ and NO_y, (b) precipitation (Precip.) and
 901 solar radiation (SR), (c) wind speed (WS) and pressure (P), and (d) relative humidity
 902 (RH) and temperature (T). The WS at the heights of 8 m (solid gray circles) and 240 m
 903 (solid black circles) are shown in (c).



904
 905 | **Figure** Fig. 3. Time series of NR-PM₁ species for the entire year. The pie charts show the
 906 average chemical composition of NR-PM₁ during the four seasons (summer, fall, winter
 907 and spring).

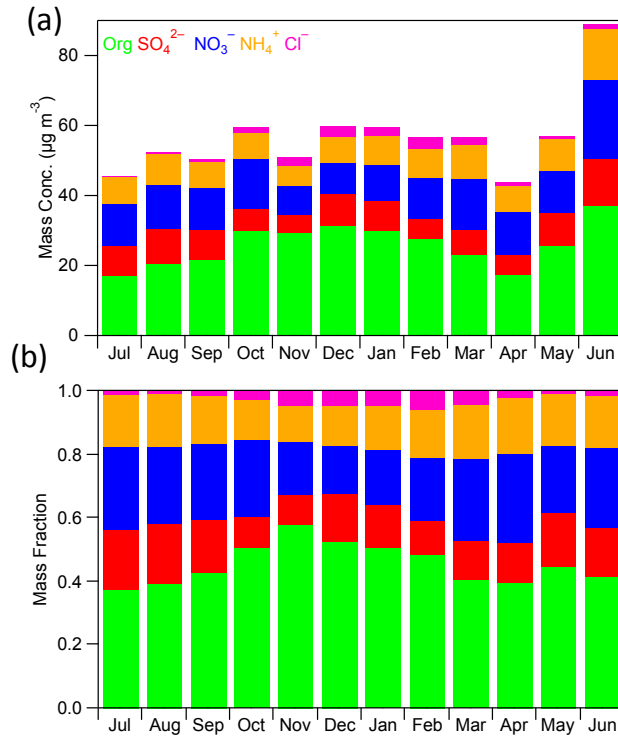


908
 909 | **Figure** Fig. 4. Frequency of NR-PM₁ mass loadings during the four seasons: (a) summer;
 910 (b) fall; (c) winter; (d) spring. **Note that the frequency was calculated with 15 min**
 911 **average data.**

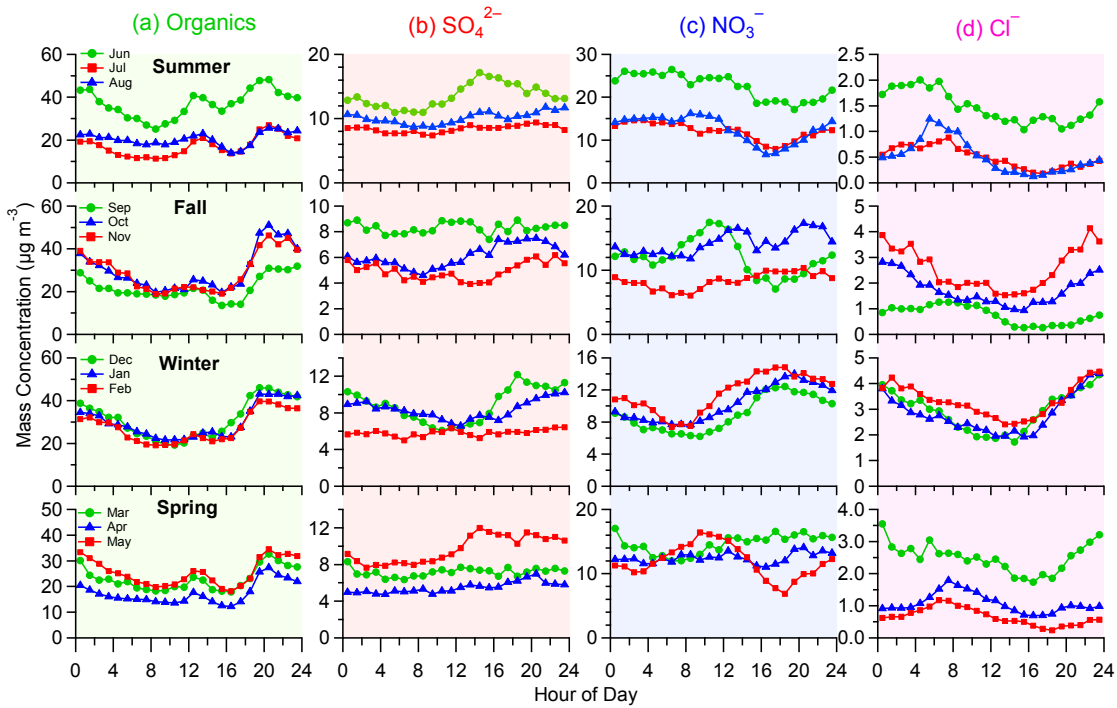


912
913

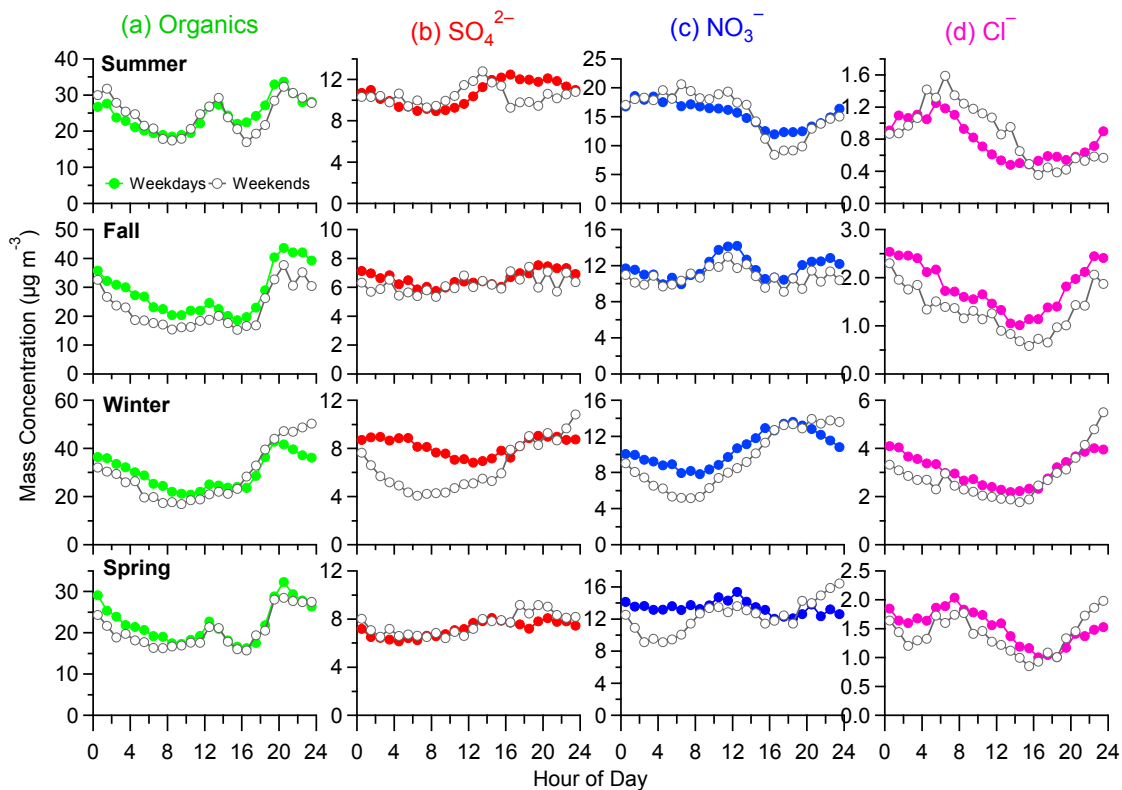
914 | **Figure** Fig. 5. Seasonal variation of non-refractory submicron aerosol species. The bars
915 represent the 25th and 75th percentiles.



916
 917 | **Figure** Fig. 6. Monthly variation of (a) mass concentrations and (b) mass fractions of NR-
 918 PM₁ species.



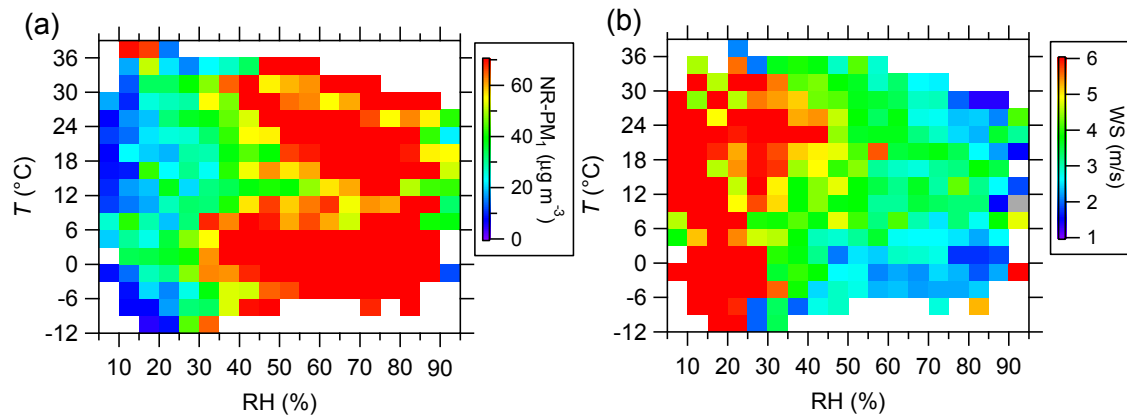
919
 920 | **Figure** Fig. 7. Monthly average diurnal cycle of (a) organics, (b) sulfate, (c) nitrate, and
 921 (d) chloride during the four seasons.



922

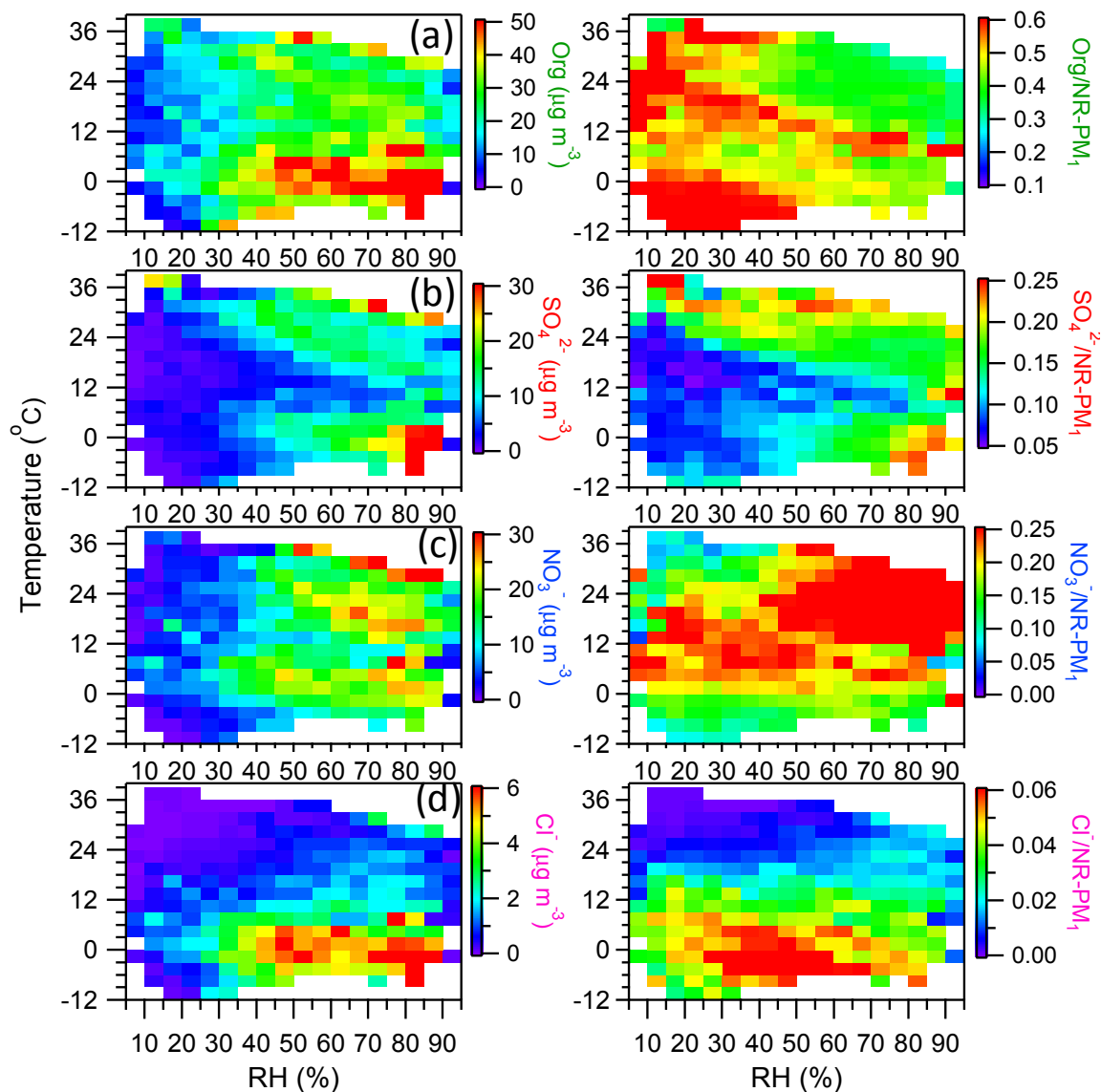
923 | **Figure** Fig. 8. Comparison of the average diurnal cycles of (a) organics, (b) SO_4^{2-} , (c)
 924 NO_3^- , and (d) Cl^- between weekdays and weekends during the four seasons. Note that the
 925 periods with $\text{NR-PM}_1 < 20 \mu\text{g m}^{-3}$ are excluded.

926

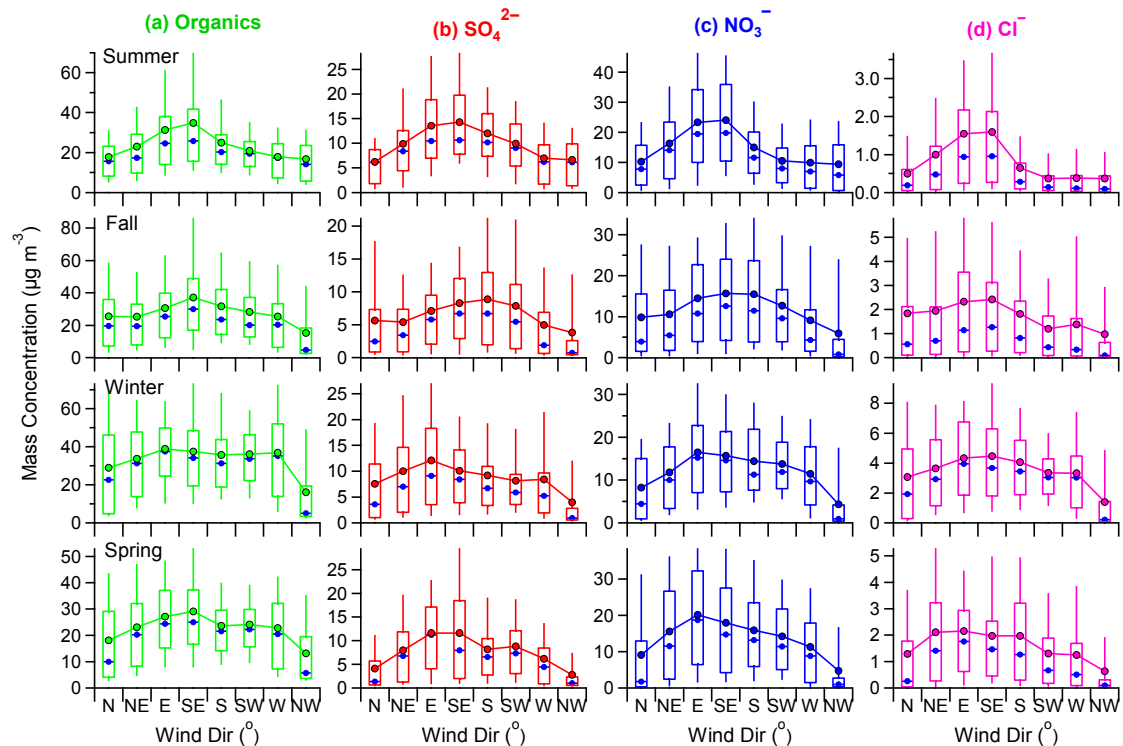


927

928 | **Figure** Fig. 9. RH/ T dependence of (a) NR-PM_1 mass concentration and (b) WS for a
 929 whole year. The data are grouped into grids with increments of RH and T being 5% and
 930 3°C , respectively. Grids with the number of data points fewer than 10 are excluded.

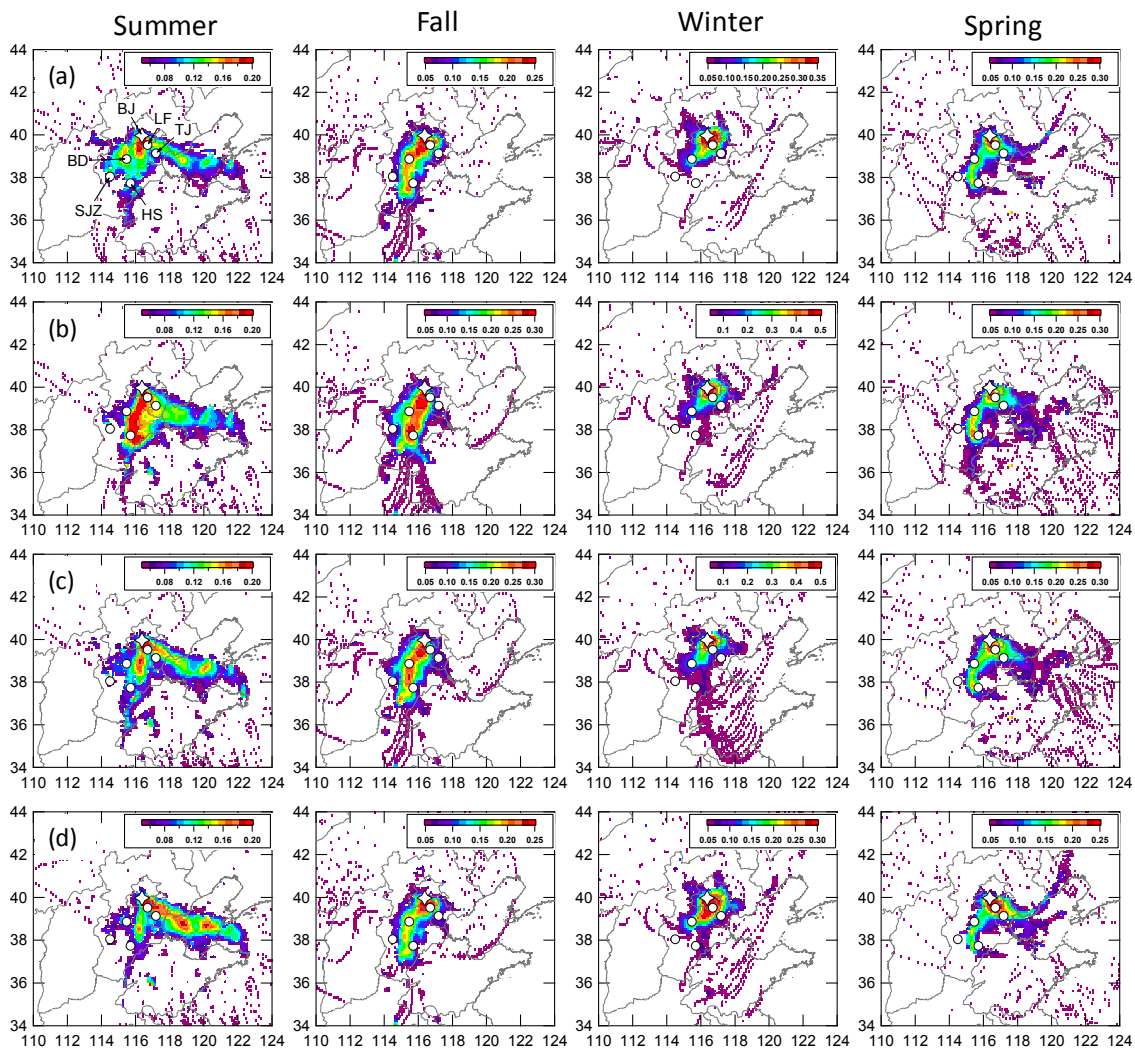


931
 932 | **Figure** Fig. 10. RH/*T* dependence of mass concentrations and mass fractions of aerosol
 933 species for a whole year: (a) organics; (b) sulfate; (c) nitrate; (d) chloride. The data are
 934 grouped into grids with increments of RH and *T* being 5% and 3°C, respectively. Grids
 935 with the number of data points fewer than 10 are excluded.



936

937 | **Figure** Fig. 11. Box plots of mass concentrations of (a) organics, (b) SO_4^{2-} , (c) NO_3^- , and
 938 (d) Cl^- as a function of wind directions sectors. All the data were segregated into eight
 939 wind sectors representing north (N), northeast (NE), east (E), southeast (SE), south (S),
 940 southwest (SW), west (W), and northwest (NW). The mean (cross), median (horizontal
 941 line), 25th and 75th percentiles (lower and upper box), and 10th and 90th percentiles
 942 (lower and upper whiskers) are shown.



943

944 | **Figure** Fig. 12. PSCF of NR-PM₁ species during four seasons: (a) organics; (b) sulfate; (c)
 945 nitrate; (d) chloride. The cities marked in each panel are Beijing (BJ), Tianjing (TJ),
 946 Langfang (LF), Baoding (BD), Shijiazhuang (SJZ), and Hengshui (HS). The color scales
 947 indicate the values of PSCF.